isome proliferator-activated receptor γ (PPARγ), which is expressed at high levels in adipocytes, forms a heterodimeric DNA-binding complex with retinoid X receptor, and acts as a transcriptional regulator of genes involved in adipocyte lipid metabolism. One such reagent, troglitazone, was reported to reduce the excessive islet triglyceride (TG) content of Zucker diabetic fatty (ZDF fa/fa) rats, which led to the restoration of β-cell function and the prevention of lipoapoptosis of β cells.[5,6] Troglitazone has also been shown to reduce TG content in liver and heart of prediabetic ZDF rats[6] or to reduce hepatic TG contents concurrently with improvement of plasma levels of TG and insulin in ZDF fa/fa rats suggesting restoration of SREBP-1 gene expression.[7] To examine effectiveness of thiazolidinediones on the experimental hepatic steatosis caused by chronic ethanol administration, we have herein chosen pioglitazone, another derivative of the antidiabetic reagents; this compound has never been reported so far to cause lactic acidosis or to increase transaminases, whereas troglitazone was withdrawn from the market after a case report of severe hepatic failure.[8] Our attempt to examine the hypothesis in this study has not only shown the effectiveness of pioglitazone but also shed light on significance of the c-Met–mediated signaling pathway to regulate synthesis and removal of triglycerides as a potential therapeutic target for treatment of ethanol-induced hepatic steatosis and injury.

Materials and Methods

Animal Feeding

The Lieber–DeCarli diets were purchased from Bio-Serv, Inc (Frenchtown, NJ).[9] Four-week-old male Sprague–Dawley rats housed in temperature- and light-controlled rooms were randomly divided into 3 groups: (A) rats fed ethanol-containing liquid diet for 6 weeks (n = 9), (B) rats pair fed ethanol-containing liquid diet for 6 weeks during which they were given pioglitazone (10 mg/kg body weight per day) once every 24 hours intragastrically (n = 9), and (C) rats pair fed isocaloric liquid diet without ethanol for 6 weeks (n = 9). Pioglitazone was dissolved in methylcellulose before use. Maeshida et al.[10] reported that pioglitazone was well absorbed from the gastrointestinal tract at an extent of 96% in rats. The plasma concentration of pioglitazone peaked at 4 hours after dosing and declined with a half-life of 2.6 hours. They also showed the concentration of radioactivity in rat tissues at 0.5, 2, 6, 10, 24, and 72 hours after oral administration of [^{14}C]pioglitazone.[10] The radioactivity of liver tissue was higher than that of plasma, and it peaked at 6 hours. The concentration of pioglitazone in liver at 24 hours after oral administration is still about one third of the concentration at 30 minutes. There is another report describing that 1 dose of 10 mg/kg of pioglitazone every 24 hours ameliorated insulin resistance associated with diabetes in rats.[11] Based on these previous papers, we think it reasonable to expect that 1 dose of 10 mg/kg of pioglitazone every 24 hours is sufficient to sustain effective concentration. The rats in groups A and C were given methylcellulose once every 24 hours intragastrically for 6 weeks in the same amount as their corresponding litter mates in group B. The rats in group B and group C were pair fed daily on an isoenergetic basis with the corresponding litter mates fed the ethanol-containing diet (group A). To investigate whether another thiazolidinedione, troglitazone, could prevent alcoholic fatty liver, we next gave troglitazone (200 mg/kg body weight/day) to 8-week-old male SD rats (n = 6), instead of pioglitazone, in the same way as our last examination of pioglitazone. Troglitazone was also well absorbed from the gastrointestinal tract, and the highest uptake by the liver was shown in rats.[12] All animals received humane care in compliance with the National Research Council's criteria outlined in the "Guide for the Care and Use of Laboratory Animals" prepared by the U.S. National Academy of Sciences and published by the U.S. National Institutes of Health.

Biochemical and Histological Analysis

Hepatic triglyceride contents were measured as previously described.[13] For histological analysis, liver tissue was fixed in 4% paraformaldehyde and embedded in paraffin. Alternatively, hepatic lipids were stained by an oil red O method (Nacalai Tesque Inc., Kyoto, Japan). For protein or RNA analysis, tissue was frozen in liquid nitrogen and stored at −80°C until used. Apoptosis was analyzed with TUNEL staining (Apoptosis Detection System, Promega Corp., Madison, WI) according to the manufacturer's instructions. At least 2 individual livers were examined in each group by counting the density of the positive-staining hepatocytes in 5 random × 200 fields/liver. Serum concentrations of alanine aminotransferase (ALT), aspartate aminotransferase (AST), triglyceride, total cholesterol, phospholipids, total proteins, albumin, and free fatty acids were measured with a standard clinical autoanalyzer (Hitachi 7170; Hitachi Ltd., Tokyo, Japan). Plasma glucose was measured by the glucose oxidase method with a glucose analyzer II (Beckman Instruments, Brea, CA). Plasma TG levels were measured with a GPO-Trinder triglyceride kit (Sigma, St. Louis, MO). Plasma leptin and insulin were assayed with Linco leptin and insulin assay kits (Linco Research Immunoassay, St. Charles, MO). Serum low-density lipoprotein cholesterol was measured by the direct enzymatic method[14] with Cholestest LDL (Daiichi Pure Chemicals Co., Ltd, Tokyo, Japan). Serum very low–density lipoprotein (VLDL) cholesterol was separated by a modification of the method of Hatch and Lees.[15] A commercially available enzyme-linked immunosorbent assay kit was used to determine serum tumor necrosis factor-α (TNF-α).

Table 1. Primer and Taqman Probe Sequences for Real-Time PCR

Gene	Sense primer (5'-3')	Antisense primer (5'-3')	Taqman probe (5'-3')
c-Met	5'-CGACATTCAGTCCGAGGTTCA-3'	5'-GGGACACTGGCCTGACTCTTC-3'	5'-TGCATGTTCTCCCCACTTGCGG-3'
HGF	5'-GACATGTCTTGCCTGATTCTGTGT-3'	5'-AGTCTGTGACATTCCTCAGTGTTCA-3'	5'-TCACCGTTGCAGGTCATGCATTCA-3'
HOX1	5'-CACCTTCCCGAGCATCGA-3'	5'-AGGCGGTCTTAGCCTCTTCTGT-3'	5'-CTCGCATGAACACTCTGGAGATGACC-3'
MT1	5'-CTGCTCCACCGGCGG-3'	5'-GCCCTGGGCACATTTGG-3'	5'-CTCCTGCAAGAAGAGCTGCTGCTCCT-3'
MT2	5'-TCCTGTGCCACAGATGGATC-3'	5'-GTCCGAAGCCTCTTTGCAGA-3'	5'-AAAGCTGCTGTTCCTGCTGCCCC-3'
SREBP1a	5'-ACACAGCGGTTTTGAACGACA-3'	5'-GCATCAAATAGGCCAGGGAA-3'	5'-CATGCTTCAGCTCATCAACAACCAAG-3'
SREBP1c	5'-GGAGCCATGGATTGCACATT-3'	5'-GCATCAAATAGGCCAGGGAA-3'	5'-CATGCTTCAGCTCATCAACAACCAAG-3'
SCD1	5'-CCTCATCATTGCCAACACCAT-3'	5'-AGCCAACCCACGTGAGAGAA-3'	5'-TTCTCTGAGACACACGCCGACCCTC-3'
SCD2	5'-ACCGCTGGCACATCAACTTC-3'	5'-GGACACCCTCTTCCGGTCAT-3'	5'-CCACGTTCTTCATCGACTGCATGGC-3'

Real-Time Quantitative PCR Analysis

Total RNA was extracted from the liver with ISOGEN (Nippon Gene, Tokyo, Japan) according to the method of Chomczynski and Sacchi, as previously described.[16] For the reverse-transcriptase reaction, TaqMan reverse transcription reagents (Applied Biosystems, Foster City, CA) were used. Briefly, the reverse-transcriptase reaction (final volume of 50 μL) was conducted for 60 minutes at 37°C followed by 25°C for 10 minutes using random hexamers. Polymerase chain reaction (PCR) amplification was performed with TaqMan Universal Master Mix (Applied Biosystems). In brief, reactions were performed in duplicate containing 2× Universal PCR master mix, 2 μL of template cDNA, 900 nmol/L of primers, and 250 nmol/L of probe in a final volume of 50 μL and were analyzed in a 96-well optical reaction plate (Applied Biosystems). Primers and probes were synthesized by Applied Biosystems custom oligo synthesis service. Sequences of primers and probes are shown in Table 1. Probes include a fluorescent reporter dye, FAM, on the 5′ end and labeled with fluorescent quencher dye, TAMRA, on the 3′ end to allow direct detection of the PCR product. Reactions were amplified and quantified using an ABI 7700 sequence detector and manufacturer's software (Applied Biosystems). The threshold cycle (Ct) indicates the fractional cycle number at which the amount of amplified target reaches a fixed threshold. The relative quantity of target messenger RNA (mRNA) was obtained using the comparative Ct method and was normalized using predeveloped TaqMan assay reagent rat 18S ribosomal RNA as an endogenous control (Applied Biosystems) (for details, see user Bulletin 2 for the ABI PRISM 7700 Sequence Detection System under www.appliedbiosystems.com/support/tutorials). Briefly, the TaqMan software (Applied Biosystem) was used to calculate a Ct value for each reaction, where the Ct value is the point in the extension phase of the PCR reaction that the product is distinguishable from the background. The Ct values were then normalized for amplification by subtracting the Ct value calculated for 18S ribosomal RNA, an endogenous control for the amount of mRNA from the same sample, to obtain a Ct using the following equation: Ct target − Ct 18S ribosomal RNA = Ct. The fold induction was calculated relative to the Ct value obtained in the control rats or cells. The normalized expression was calculated as fold changes in a quantity of mRNA. TNF-α mRNA was measured using predeveloped TaqMan assay reagent rat TNF-α (Applied Biosystems) (for details, see user Bulletin 2 for the ABI PRISM 7700 Sequence Detection System under www.appliedbiosystems.com/support/tutorials).

Isolation and Primary Culture of Rat Hepatocytes

Primary cultured hepatocytes were prepared from livers of ethanol-fed rats through a collagenase perfusion method in group A as described elsewhere.[17] The isolated hepatocytes were cultured on gelled pig tendon collagen (Cellmatrix, Nitta zerachin, Ltd., Osaka, Japan), and the second layer of collagen gel was spread over the cells after 1 day of incubation as previously described.[17] A PPARγ-selective agonist AD4833 (pioglitazone hydrochloride, Takeda, Ltd., Osaka, Japan)[18] and troglitazone (Sankyo, Ltd., Tokyo, Japan)[5] was dissolved in dimethyl sulfoxide (DMSO) and added to the hepatocytes at various doses in a volume at 0.05% of the medium. In the control, the medium was supplemented with the same volume of DMSO.

Transcriptome Analyses by DNA Microarray

Transcriptome analyses were performed by using DNA microarrays (Atlas cDNA expression arrays, Clontech). Preparation of ^{33}P-labeled cDNA samples, hybridization, and washing were carried out with total RNA of the liver tissue according to the manufacturer's manual. All data sets were normalized to the signal density of housekeeping genes, such as the gene encoding glyceraldehyde-3-phosphate dehydrogenase, and total radioactivity, which represents the total amount of cDNA hybridized to the microarrays. The threshold for determining the significance of changes in the level of gene expression was established by using an algorithm that requires both a significant absolute and significant fold change.[19,20]

Western and Immunoprecipitation Analysis

Total cellular protein (50 μg) collected from snap-frozen liver was subjected to Western blot analysis for c-Met, mature hepatocyte growth factor (HGF), and apolipoprotein B (apoB)100. For immunoblot analyses, primary antisera were used at the concentration of 1:100. The membranes were

probed with antirat c-Met antibody (Santa Cruz Biotechnology, Santa Cruz, CA), anti-rat HGFα antibody (Santa Cruz Biotech), and anti-rat apoB antibody (Santa Cruz Biotech). For immunoprecipitation, lysates (10 mg of protein) were incubated with protein A-agarose beads (Pierce, Rockford, IL) to precipitate the antigen-antibody complex. Samples were separated by SDS-PAGE on 10% polyacryamide gels. After electrophoresis, the gel was transferred to polyvinylidine difluoride sheets, which were subsequently probed with anti-phosphotyrosine antibody (PY-20; ICN Biomedicals Inc., Aurora, OH) or antirat c-Met antibody. Then, they were incubated with a chemiluminescence substrate (ECL reagent: Amersham Life Science, Buckinghamshire, UK) and exposed to Hyperfilm-MP (Amersham). Densitometric analysis was performed with National Institutes of Health Image Data analysis software.

Immunohistochemistry

For detection of 4-hydroxynonenal (4-HNE) protein adducts, paraffinized sections were deparaffinized, rehydrated, treated with normal horse serum, and incubated with mAb anti-4-HNE (0.625 μg/mL) (Nippon Rouka Seigyo Kenkyuujo, Tokyo, Japan) overnight at 4°C. After several washes with phophate-buffered saline, the sections were stained with biotinylated antimouse IgG for 1 hour (Vectastain Elite ABC kit; Vector Laboratories, Inc., Burlingame, CA). To prevent endogenous peroxidase reactions, the samples were pretreated with 0.3% H_2O_2 in cold methanol for 30 minutes and were subsequently incubated with avidin and horseradish peroxidase (HRP)-conjugated biotin for 30 minutes, followed by detection with 3,3′-diaminobenzidine solution containing 0.003% H_2O_2.

Measurement of DNA Synthesis

DNA synthesis was measured by bromodeoxyuridine (BrdU) incorporation with a Cell Proliferation ELISA, BrdU kit (Roche Molecular Biochemicals, Mannheim, Germany). In brief, hepatocytes were suspended in William's medium E supplemented with 10% fetal bovine serum (FBS), 10 nmol/L insulin, 10 nmol/L dexamethasone, penicillin (5 U/mL), and streptomycin (50 μg/mL) and seeded at a density of 5×10^4 cells/cm^2 on collagen-coated dishes. The culture medium was exchanged after 4 hours for William's medium E supplemented with 10% FBS. After incubation in William's medium E with 10% FBS for approximately 20 hours, the culture medium was exchanged for William's medium E containing 10% FBS with HGF/SF, pioglitazone, or both. They were then cultured for another 24 hours with the addition of BrdU and were harvested in determining the BrdU incorporation into cellular DNA according to the manufacturer's instructions.

Analyses for Effects of Pioglitazone on Ethanol Metabolism in Rats

Four-week-old male Sprague–Dawley rats were randomly divided into 2 groups: rats fed the Lieber–DeCarli control liquid diet for 10 days (n = 16) and those pair fed isocaloric control liquid diet for 10 days during which they were given pioglitazone (10 mg/kg body weight/day) once every 24 hours intragastrically (n = 16). After overnight starvation, rats were given ethanol intragastrically at 4 g/kg body weight on the 10th day. Before and 2, 12, and 24 hours after the ethanol administration, 4 rats in each group were sacrificed to collect heparinized blood samples which were immediately deproteinized to determine ethanol and acetaldehyde concentrations through gas chromatography.[21]

Statistical Analysis

All data are expressed as the mean ± standard error. Statistical analysis was performed by using the unpaired Student *t* test or by 1-way analysis of variance. When the analysis of variance analyses were applied, differences in mean values among groups were examined by Fisher's multiple comparison test.

Results

Pioglitazone Attenuates Hepatic Steatosis Caused by Chronic Ethanol Administration

The hepatic triglyceride concentration in rats given the isocaloric pair fed liquid diet was 9.67 (±4.34) mg/g liver weight, as opposed to 78.24 (±11.25) mg/g liver weight in the rats given the ethanol-containing diet for 6 weeks (Table 2). Histological analysis showed that lipid droplets accumulated in the hepatocytes in pericentral regions but not in those in periportal regions in the ethanol-fed rats. On the other hand, such changes were not notable in the control liver even with the lipid-specific oil red staining (Figure 1). Pioglitazone (10 mg/kg per day) markedly decreased accumulation of lipid droplets in both perivenular and the periportal regions with the total body weight remaining unchanged (Figure 1). In good agreement with these results, hepatic triglyceride levels became as low as in the pair-fed control rats (Table 2). Treatment with methylcellulose as a vehicle had no effect on either triglyceride contents or histology in the liver (data not shown). The ethanol feeding caused an increase in the liver weight/body weight ratio and a decrease in the epididymal fat weight/body weight ratio, whereas pioglitazone treatment prevented these changes (Table 2).

Analyses of serum AST and ALT activity to assess the effect of pioglitazone on liver function showed that pioglitazone suppressed the elevation of serum concentrations of AST and ALT in ethanol-fed rats (Table 2), and this improvement was associated with improvement in histological findings in the liver. Ethanol feeding caused elevations of the serum concentrations of free fatty acids,

Table 2. Body Weight and Serum Biochemical Parameters in the Treated Groups

	Ethanol (n = 8)	Ethanol + Pioglitazone (n = 8)	Control (n = 8)
Liver weight/body weight (%)	[b]3.57 (0.34)	3.08 (0.24)	2.35 (0.25)
Epididymal fat weight/body weight (%)	[a]0.574 (0.044)	0.808 (0.065)	0.806 (0.062)
Liver triglyceride (mg/g liver weight)	[a]78.24 (11.25)	14.36 (3.72)	9.67 (4.34)
AST (IU/L)	[a]362.4 (25.4)	195.7 (23.3)	38.1 (10.6)
ALT (IU/L)	[a]174.2 (13.4)	50.3 (4.9)	33.5 (5.2)
Phospholipid (mg/dL)	159.2 (10.8)	146.7 (14.2)	110.0 (7.3)
FFA (mEQ/L)	0.562 (0.126)	0.550 (0.240)	[a]0.448 (0.066)
Total cholesterol (mg/dL)	116.0 (8.9)	130.8 (20.9)	[a]72.7 (7.1)
LDL (mg/dL)	82.4 (15.8)	98.0 (22.3)	45.4 (7.9)
VLDL (mg/dL)	7.25 (0.23)	7.96 (0.35)	6.94 (0.28)
Triglyceride (mg/dL)	21.67 (3.68)	20.35 (2.76)	[a]14.58 (2.64)
Leptin (ng/mL)	0.62 (0.25)	1.55 (1.25)	0.82 (0.46)
TNF-α (pg/mL)	22.26 (4.48)	23.32 (3.87)	25.02 (4.87)

NOTE. Results (and standard error of the mean) from 8 rats/group at the end of feeding period.
[a]$P < 0.05$ versus both other groups.
[b]$P < 0.05$ versus the control group.

triglyceride, phospholipid, total cholesterol, and LDL, and pioglitazone caused elevation of serum VLDL levels, but no significant changes were found in serum TNF-α or leptin levels (Table 2). We did not find any significant changes in total protein, albumin, glucose, insulin, lactic acid, or choline esterase levels (data not shown).

Transcriptome Analyses for Mining Genes Responsible for Antisteatotic Effects of Pioglitazone

To elucidate mechanisms by which pioglitazone reduces hepatic lipid contents in alcoholic fatty liver, we

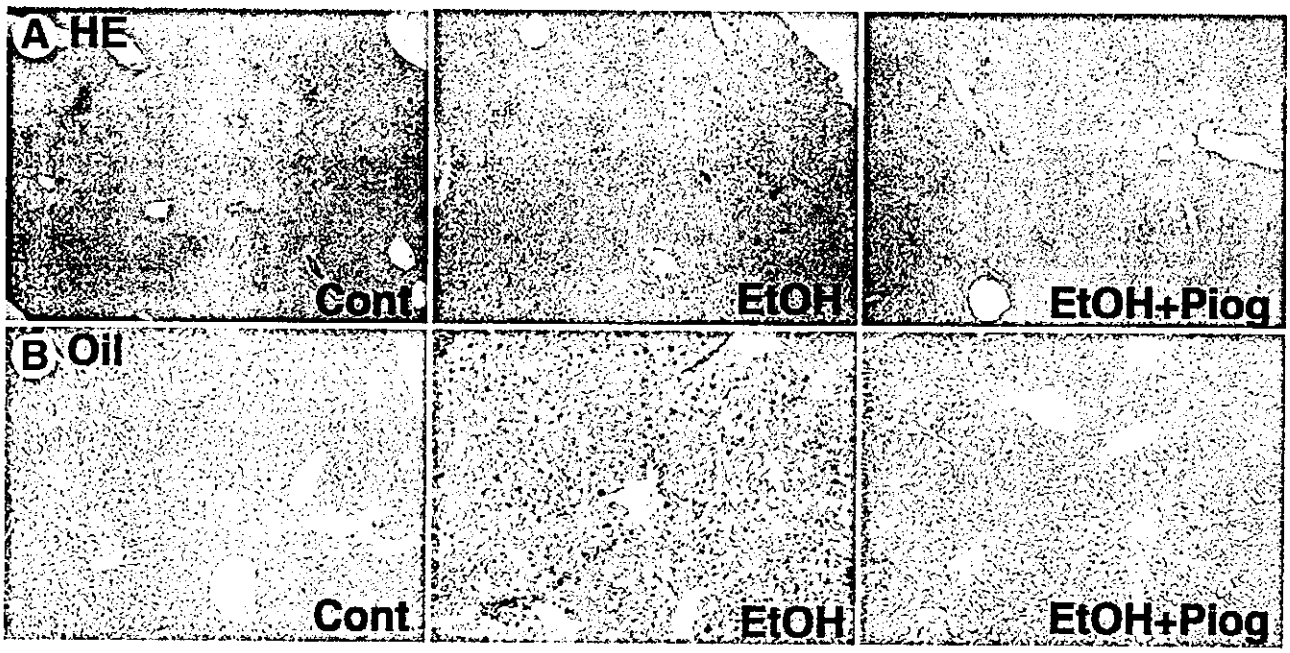

Figure 1. Effect of pioglitazone on liver histology in the ethanol-fed rats. (*A*) H&E-stained sections of representative liver samples of control rats (Cont), ethanol-fed rats (EtOH), and ethanol-fed rats given pioglitazone (EtOH+Piog) (×40). Minimal steatosis or no change was seen in the livers of the pair-fed control rats. Severe macrovesicular steatosis was observed preferentially in the perivenular areas in the ethanol-fed rats. Pioglitazone markedly decreased accumulation of lipid droplets in both the perivenular and the periportal areas. Only minimal steatosis was left in the livers of ethanol-fed rats given pioglitazone. (*B*) Oil red–stained sections of representative liver samples of control rats, ethanol-fed rats, and ethanol-fed rats given pioglitazone (×40). Specific staining of lipid accumulation was shown. Pioglitazone markedly decreased accumulation of lipid droplets.

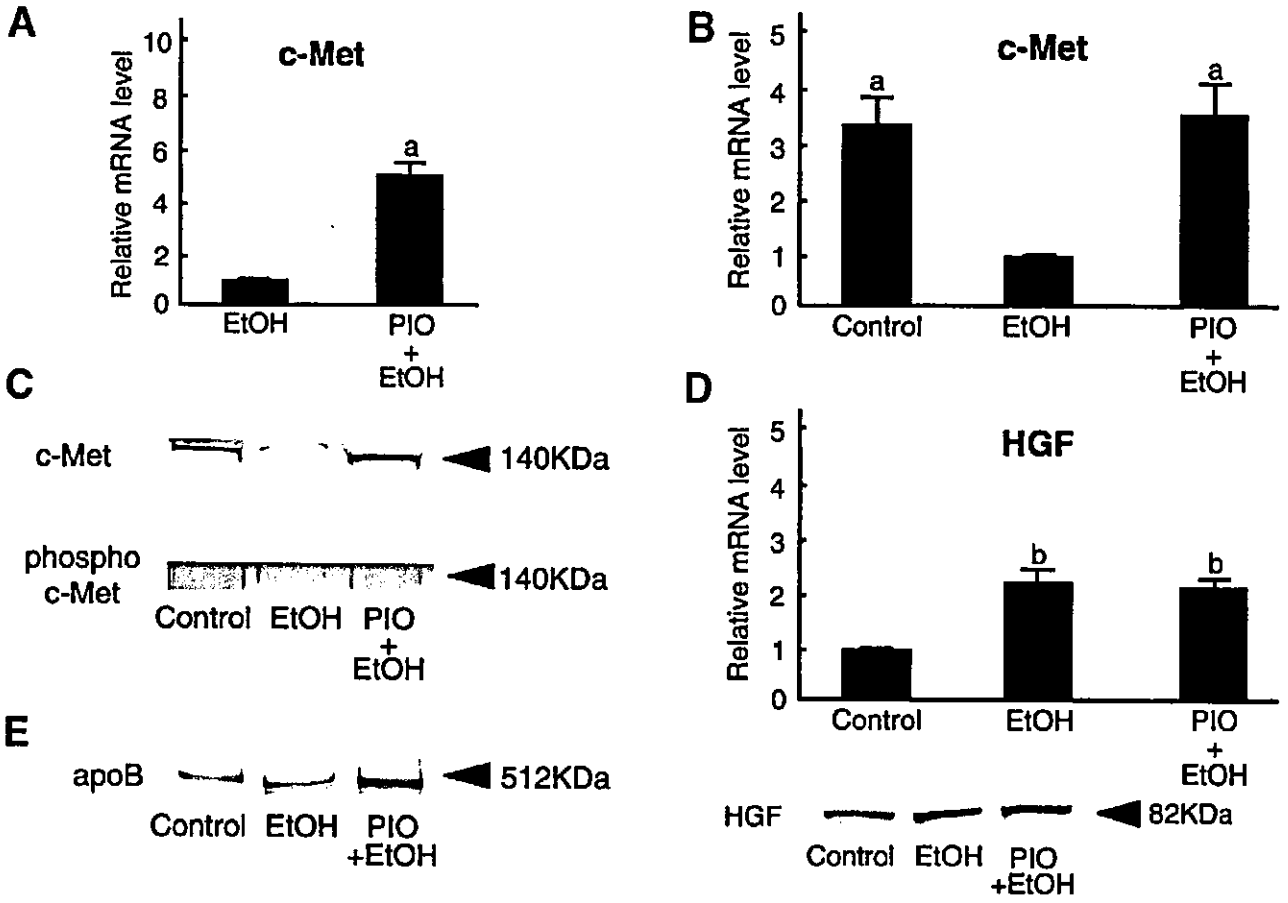

Figure 2. Hepatic c-Met, HGF, and apoB expression. (*A*) DNA microarray analysis showed that pioglitazone increased hepatic c-Met mRNA expression. Results (and standard error of the mean) from 3 rats/group at the end of feeding period. $^{a}P < 0.05$ versus the ethanol-fed group. EtOH, ethanol-fed rats; PIO+EtOH, ethanol-fed rats given pioglitazone. (*B*) Real-time PCR analysis showed that chronic ethanol feeding decreased hepatic c-Met expression and that pioglitazone prevented this decrease. Results (and standard error of the mean) from 6 rats/group at the end of feeding period. All real-time quantitative PCR reactions were carried out in duplicate. $^{a}P < 0.05$ versus the ethanol-fed group. (*C*) Western immunoblot analysis of expression of c-Met (*upper*) and tyrosine phosphorylation of c-Met (*lower*) in liver homogenates (containing 50 μg of total protein each). (*D*) Real-time PCR analysis (*upper*) and Western blotting analysis (*lower*) showed that chronic ethanol feeding increased hepatic HGF expression and pioglitazone had no effect on this. Results (and standard error of the mean) from 6 rats/group at the end of feeding period. All real-time quantitative PCR reactions were carried out in duplicate. $^{b}P < 0.05$ versus the control group. (*E*) Western immunoblot analysis of expression of apoB in liver homogenates (containing 50 μg of total protein each). Control, rats pair-fed isocaloric liquid diet without ethanol; EtOH, ethanol-fed rats; PIO+EtOH, ethanol-fed rats given pioglitazone.

applied DNA microarrays to reveal differential mRNA expression between the livers exposed to chronic ethanol feeding with and without pioglitazone treatment. The transcriptome analysis allowed us to reveal up-regulation of c-Met (Figure 2*A*) and down-regulation of SCD-1 and -2, lipogenic enzymes in the liver (data not shown). Pioglitazone had no effect on the hepatic levels of TNF-α, UCP-2, CYP4A2 (cytochrome P450 4A2), CYP2E1, PPARγ, AMPK-catalytic subunit (α1 and α2), microsomal triglyceride transfer protein (MTTP), hepatic enzymes contributing to fatty acid oxidation such as carnitine palmitoyltransferase-1 or acyl-CoA oxidase (data not shown). These results were confirmed by real-time PCR analysis (Table 3). Chronic ethanol feeding significantly increased CYP2E1 mRNA and decreased PPARγ mRNA (Table 3).

Pioglitazone Increased Hepatic c-Met Expression and Induced Tyrosine Phosphorylation of c-Met Leading to Increased Hepatic apoB Expression

Alterations in c-Met gene expression were also confirmed at the protein levels. Moderate expression of c-Met protein was observed in the liver of the control rats, and the ethanol diet decreased the expression of c-Met protein (Figure 2*C*). The decrease in c-Met protein

Table 3. The Level of Expression of Genes Known to Play a Role in the Formation of Steatosis and Steatohepatitis Among the Treated Groups

Gene	Ethanol	Ethanol + Pioglitazone
TNF-α	1.12 ± 0.22	1.17 ± 0.23
UCP2	1.21 ± 0.30	1.18 ± 0.21
CYP2E1	[a]1.81 ± 0.32	[a]1.76 ± 0.24
CYP4A2	1.07 ± 0.36	1.11 ± 0.23
PPAR-α	[a]0.46 ± 0.12	[a]0.50 ± 0.09
AMPKα1	0.89 ± 0.31	0.95 ± 0.19
AMPKα2	1.14 ± 0.15	1.08 ± 0.17
Acyl-CoA oxidase	0.90 ± 0.28	0.95 ± 0.21
CPT-1	1.06 ± 0.17	1.10 ± 0.23
MTTP	0.94 ± 0.27	0.95 ± 0.26

NOTE. Results (and SEM) from 8 rats/group at the end of feeding period. Quantifications were normalized for RNA from the liver in the control group.
[a]$P < 0.05$ versus the control group.

in the liver of the ethanol-fed rats was restored by pioglitazone administration (Figure 2*C*). The level of tyrosine phosphorylation of c-Met was also reduced in the ethanol-fed liver, whereas the pioglitazone treatment attenuated this change (Figure 2*C*). DNA array and real-time PCR analyses also showed that ethanol administration decreased hepatic c-Met expression and that pioglitazone prevented this decrease (Figure 2*A, B*). Chronic ethanol feeding significantly increased HGF at both mRNA and protein levels, whereas the pioglitazone treatment did not alter these levels (Figure 2*D*). Western blotting analysis showed that the level of apoB 100 protein in the liver was increased by pioglitazone in the ethanol-fed rats (Figure 2*E*).

Stimulatory Effects of Pioglitazone on c-Met Expression, Its Tyrosine Phosphorylation, DNA Synthesis, and apoB Expression in Primary-Cultured Hepatocytes

To examine the direct effect of pioglitazone on expression of c-Met, rat primary cultured hepatocytes were incubated with various doses of pioglitazone and troglitazone for 24 hours (from 24 hours to 48 hours after inoculation). Ten μM pioglitazone markedly increased c-Met expression. The same concentration of troglitazone also increased c-Met expression, and the addition of bisphenol A diglycidyl ether (BADGE), a PPARγ antagonist,[22] inhibited this reaction (Figure 3*A*). The level of tyrosine phosphorylation was also increased by the addition of pioglitazone (Figure 3*B*). Stimulation of hepatocytes with both 5 ng/mL HGF and pioglitazone led to a greater increase in DNA synthesis than with either alone. In primary-cultured hepatocytes, HGF at 5 ng/mL and pioglitazone at 10 μmol/L maximally stimulated BrdU incorporation into DNA (Figure 3*C*). Pioglitazone also mimicked stimulatory effects of HGF on the expression of apoB in primary-cultured hepatocytes as seen in Figure 3*D* and *E*.

Troglitazone Mimicked the Actions of Pioglitazone In Vivo

In the in vivo study for troglitazone, we found that troglitazone significantly reduced fat accumulation and improved serum transaminase level in ethanol-fed rats. Troglitazone also enhanced hepatic c-Met expression (Figure 4).

Pioglitazone Decreased Hepatic SCD-1, 2, and SREBP-1c Expressions, Mimicking Effects of HGF

The real-time PCR analysis showed that chronic ethanol feeding conspicuously increased hepatic SCD-1 and 2 expressions, and that pioglitazone treatment suppressed them, consistent with the results of DNA array (Figure 5). Pioglitazone significantly decreased hepatic SREBP-1c expressions, although it had no effect on hepatic SREBP-1a level (Figure 5). Such effects of pioglitazone were also reproducible in primary-cultured hepatocytes. The HGF treatment dramatically decreased SREBP-1c and SCD-2 expressions in primary-cultured hepatocytes (Figure 6*A*). Pioglitazone treatment also decreased SREBP-1c and SCD-2 expressions upon the application of HGF, although the reagent had no effect on them without it (Figure 6*B, C*).

Pioglitazone Attenuates Hepatic Lipid Peroxidation Elicited by Chronic Ethanol Feeding

4-HNE-adducted protein, as a product of lipid peroxidation reaction, was intensely detected in centrilobular regions of ethanol-fed rats and colocalized with accumulated lipid droplets. The pioglitazone treatment decreased the products of lipid peroxidation (Figure 7*A*). We found by real-time PCR analysis that the hepatic level of stress response proteins such as metallothionein (MT) -1, -2, and heme oxygenase (HOX)-1 dramatically increased in ethanol-fed rats (group A). Pioglitazone prevented these stress responses induced by ethanol (Figure 7*B*). Of importance in the current study is that neither the pioglitazone treatment nor chronic ethanol feeding induced any notable apoptosis, as judged by the TUNEL method seen in Figure 7*C*.

In this study, all rats in the groups were pair fed daily on an isoenergetic basis, and the rats in group A and B were daily given the same amounts of ethanol. We then inquired

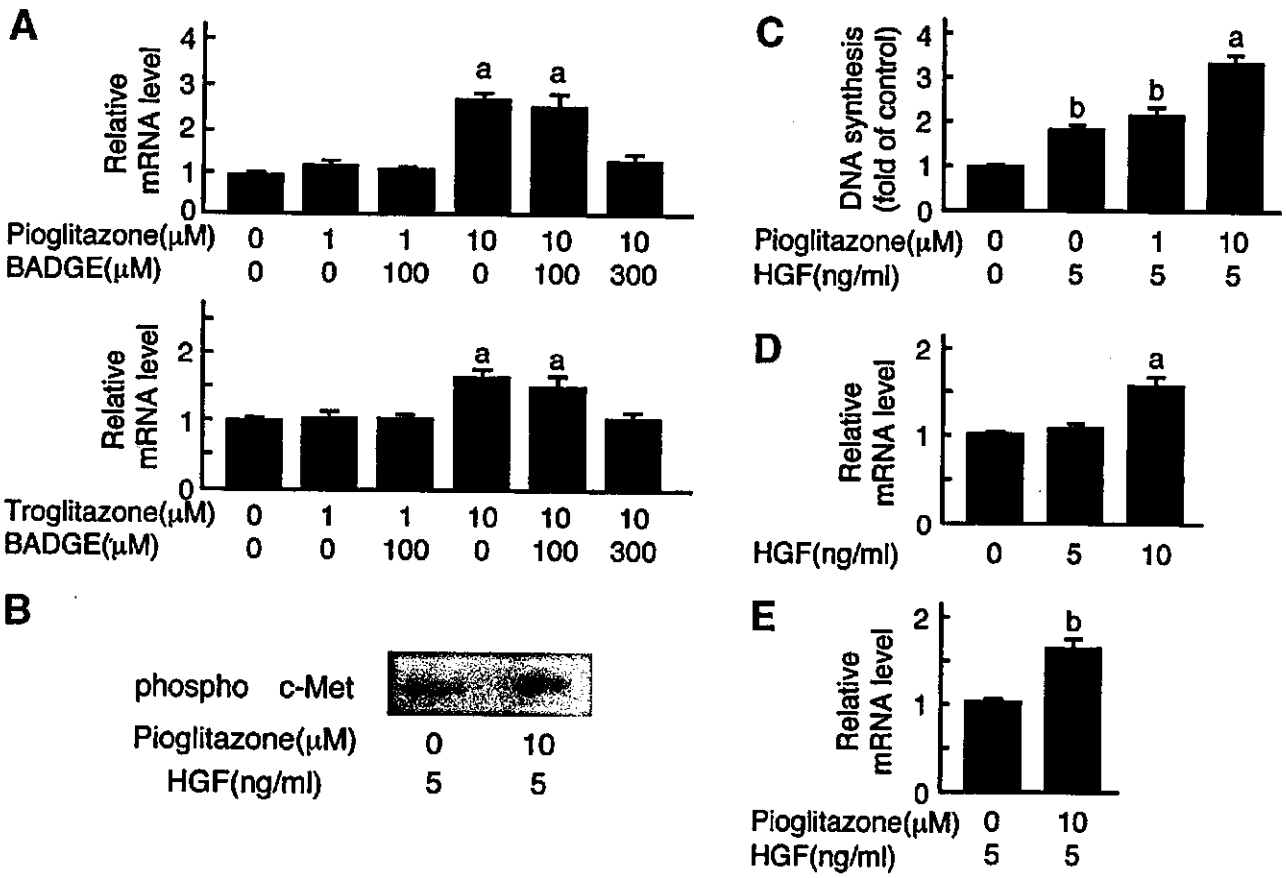

Figure 3. Direct effect of pioglitazone on expression and tyrosine phosphorylation of c-Met, expression of apoB, and on DNA synthesis in rat primary cultured hepatocytes. (*A*) Rat primary-cultured hepatocytes were incubated with various doses of pioglitazone or troglitazone for 24 hours (from 24 to 48 hours after inoculation). In the control, the medium was supplemented with the same volume of DMSO. Real-time quantitative PCR analysis of c-Met showed that 10 μmol/L of pioglitazone treatment dramatically increased c-Met expression. Ten μmol/L of troglitazone treatment also significantly increased c-Met expression. Addition of 300 μmol/L of BADGE inhibited this increase. All real-time quantitative PCR reactions were carried out in duplicate. Results (and standard error of the mean) from 4 individual experiments. $^{a}P < 0.05$ versus the groups with 0 or 1 μmol/L of pioglitazone or troglitazone treatment. (*B*) Tyrosine phosphorylation of c-Met in homogenates of primary-cultured hepatocytes stimulated or not with 5 ng/mL HGF or pioglitazone. Addition of 10 μmol/L pioglitazone induced tyrosine phosphorylation of c-Met. (*C*) Effect of pioglitazone on DNA synthesis of primary cultured hepatocytes. BrdU incorporation into cellular DNA was determined 24 hours after the addition of HGF and/or pioglitazone. $^{a}P < 0.05$ versus the other groups. $^{b}P < 0.05$ versus the groups without any addition of HGF or pioglitazone. Next, real-time PCR analysis of primary-cultured hepatocytes was used to assess apoB gene expression (*D*, *E*). (*D*) Rat primary-cultured hepatocytes were incubated with various doses of HGF for 24 hours. $^{a}P < 0.05$ versus the group without addition of HGF. (*E*) Incubation with pioglitazone with addition of 5 ng/mL of HGF for 24 hours. $^{b}P < 0.05$ versus the group without any addition of pioglitazone. All real-time quantitative PCR reactions were carried out in duplicate. Results (and standard error of the mean) from 4 individual experiments.

whether the treatment with pioglitazone by itself could alter ethanol metabolism in rats. Table 4 shows that blood levels of ethanol and acetaldehyde did not differ significantly irrespective of the presence or absence of pioglitazone in ethanol-fed rats. This result suggests that pioglitazone has little, if any, effect on ethanol metabolism and thus is not a likely mechanism for the attenuating effect of this reagent on hepatic steatosis.

Discussion

This study first suggested that pioglitazone serves as a potentially therapeutic tool to attenuate hepatic steatosis caused by chronic administration of ethanol. Furthermore, several lines of evidence provided in this study suggest that the ability of this antidiabetic to significantly alter synthesis and redistribution of lipids is ascribable to therapeutic potential against the ethanol-induced hepatic steatosis. The epididymal fat weight/body weight ratio significantly decreased in the ethanol-fed rats compared with that in the pair fed rats. Distinct from nonalcoholic hepatic steatosis, which induced by chronic alcohol abuse often coincided with energy wasting and inhibition of adipose tissue accumulation. These events are likely to result in the fact that alcoholics are

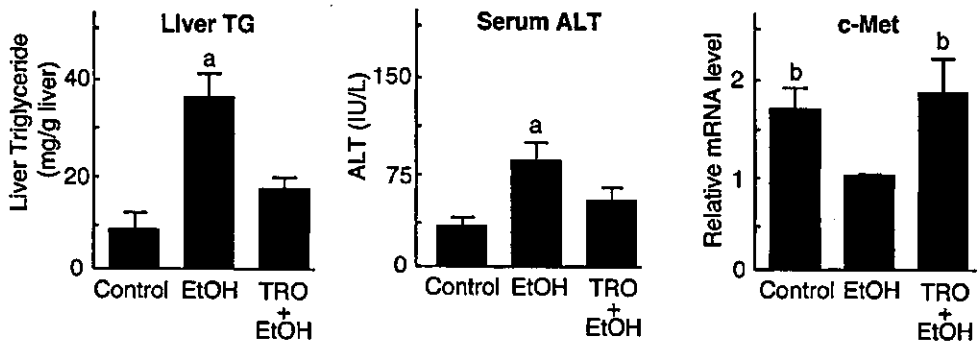

Figure 4. Troglitazone mimicked the actions of pioglitazone in vivo. Eight-week-old male SD rats fed ethanol-containing liquid diet were given troglitazone (200 mg/kg body weight per day) once every 24 hours intragastrically for 6 weeks. In this study, we divided the rats into 3 groups in the same way as our last examination of pioglitazone (n = 6). Troglitazone decreased accumulation of lipid droplets and suppressed the elevation of serum concentrations of ALT in ethanol-fed rats. Real-time PCR analyses showed that ethanol administration decreased hepatic c-Met expression and that troglitazone prevented this decrease. Results (and standard error of the mean) from 6 rats/group at the end of feeding period. All real-time quantitative PCR reactions were carried out in duplicate. $^{a}P < 0.05$ versus the other groups. $^{b}P < 0.05$ versus the ethanol-fed group. Control, rats pair-fed isocaloric liquid diet without ethanol; EtOH, ethanol-fed rats; TRO+EtOH, ethanol-fed rats given troglitazone.

not obese despite a high total energy intake.[23] Pioglitazone prevented the decrease in amount of adipose tissue, probably by mobilizing fat from the liver to adipose tissue.

It has been believed until now that impaired mitochondrial β-oxidation of fatty acids could be a major cause of triglyceride accumulation in alcoholic fatty liver.[24] In the current study, however, pioglitazone did not alter the expression of hepatic enzymes contributing to fatty acid oxidation such as carnitine palmitoyltransferase-1 or acyl-CoA oxidase (AOX) or the expression of hepatic TNF-α, uncoupling protein-2, PPARγ, or AMPK-catalytic subunit (α1 and α2) levels; plasma TNF-α, glucose, leptin, insulin levels, or insulin resistance remained unchanged. These results suggest that other mechanisms play central roles in pioglitazone's effect on alcoholic fatty liver. Differential

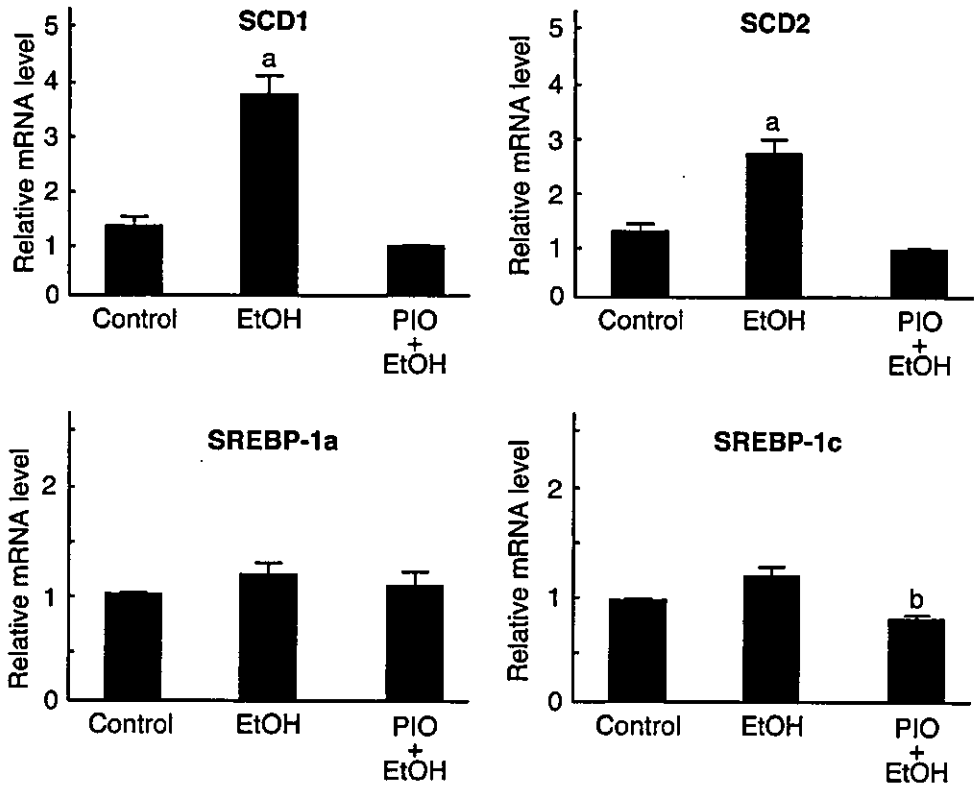

Figure 5. Hepatic SCD1, SCD2, SREBP-1a, and SREBP-1c expression. Real-time PCR analysis was carried out to quantitate hepatic mRNA levels of SCD1, SCD2, SREBP-1a, and SREBP-1c in liver homogenates among the groups. Results (and standard error of the mean) from 4 rats/group at the end of feeding period. All real-time quantitative PCR reactions were carried out in duplicate. $^{a}P < 0.05$ versus the other groups. $^{b}P < 0.05$ versus the ethanol-fed group. Control, rats pair-fed isocaloric liquid diet without ethanol; EtOH, ethanol-fed rats; PIO+EtOH, ethanol-fed rats given pioglitazone.

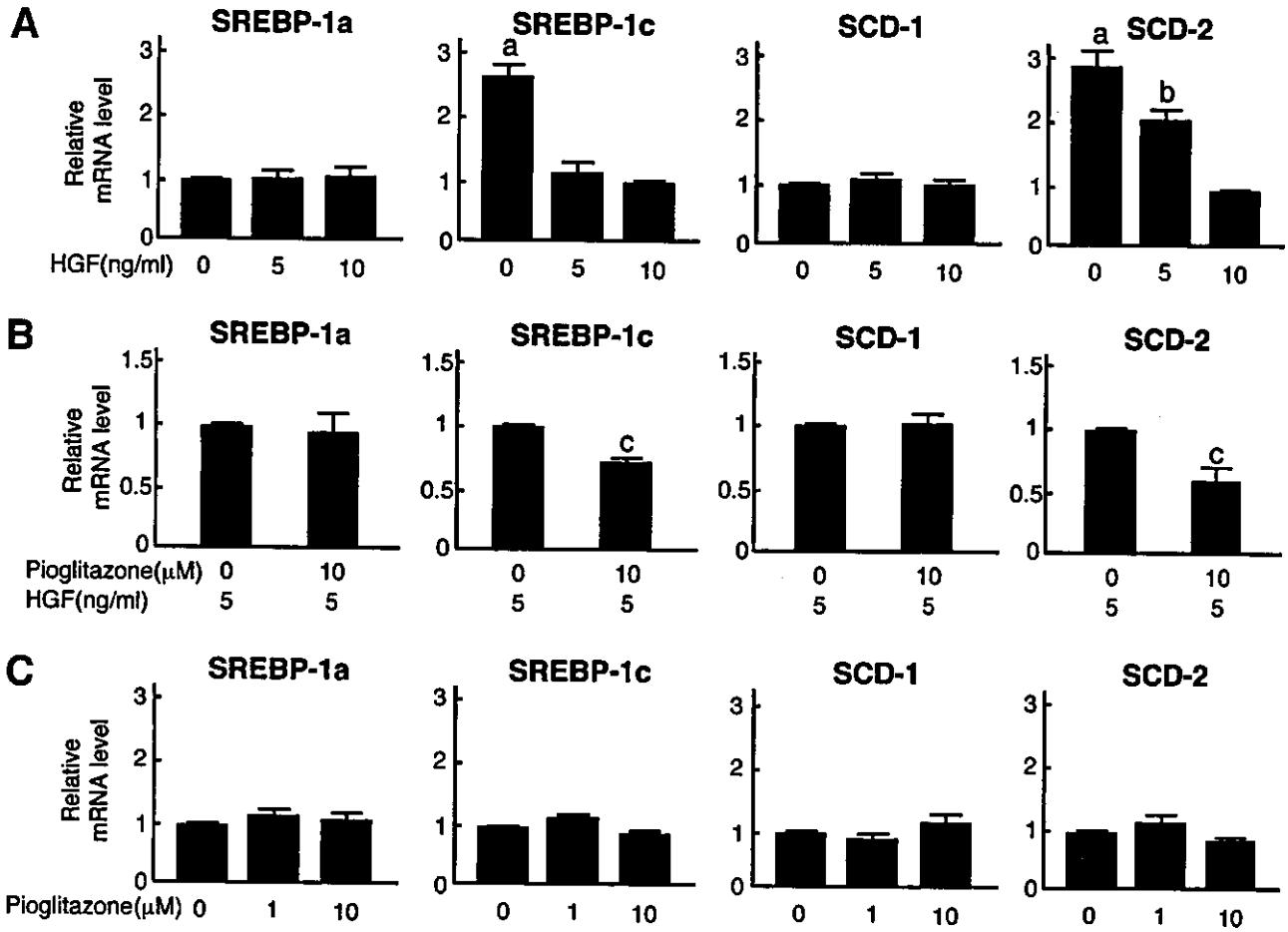

Figure 6. Effects of pioglitazone and HGF on expression of SREBP-1a, c, and SCD-1, 2 mRNA in hepatocyte cultures. Real-time PCR analysis was used to assess SREBP-1a, SREBP-1c, SCD-1, and SCD-2 gene expression. (*A*) Rat primary-cultured hepatocytes were incubated with various doses of HGF for 24 hours. $^{a}P < 0.05$ versus the other groups. $^{b}P < 0.05$ versus the group with addition of 10 ng/mL of HGF. (*B*) Incubation with pioglitazone with addition of 5 ng/mL of HGF for 24 hours. $^{c}P < 0.05$ versus the group without any addition of pioglitazone. (*C*) Incubation with various doses of pioglitazone for 24 hours. All real-time quantitative PCR reactions were carried out in duplicate. Results (and standard error of the mean) from 4 individual experiments.

transcriptome analyses comparing mRNA expression in the chronic ethanol-exposed livers with and without the pioglitazone treatment led us to pinpoint a critical role of the hepatic c-Met signaling pathway, and the results suggest that the reagent facilitates HGF-induced intracellular signaling without altering hepatic HGF levels.

HGF is the most potent stimulator of hepatocyte proliferation.[25] HGF has multiple biological properties in the liver, including mitogenic, antifibrotic, antiapoptotic, and cytoprotective activities.[26–28] Such multiple biological responses elicited by HGF are transferred through the cytoplasmic domain of c-Met, a specific cell surface transmembrane tyrosine kinase receptor.[26] Observation that pioglitazone directly enhanced both c-Met and its activated form in rat primary-cultured hepatocytes from ethanol-fed rats suggests that this reagent serves as the first clinically available tool that directly up-regulates c-Met expression in hepatocytes. Several data in the current study suggested that PPARγ is involved in mechanisms by which the reagent up-regulates c-Met, inasmuch as this event is mimicked by troglitazone, another PPARγ ligand, and is canceled by BADGE, a PPARγa antagonist. Further studies are necessary to determine the whole mechanisms for exploring direct actions of the reagent on c-Met expression.

HGF is known to stimulate apoB secretion in hepatocytes and to induce cell maturation during liver regeneration.[29] The HGF administration has recently been shown to improve alcoholic fatty liver by enhancing apoB synthesis and subsequent mobilization of lipids from hepatocytes with fatty changes.[13] These observations led us to examine if pioglitazone could serve as a

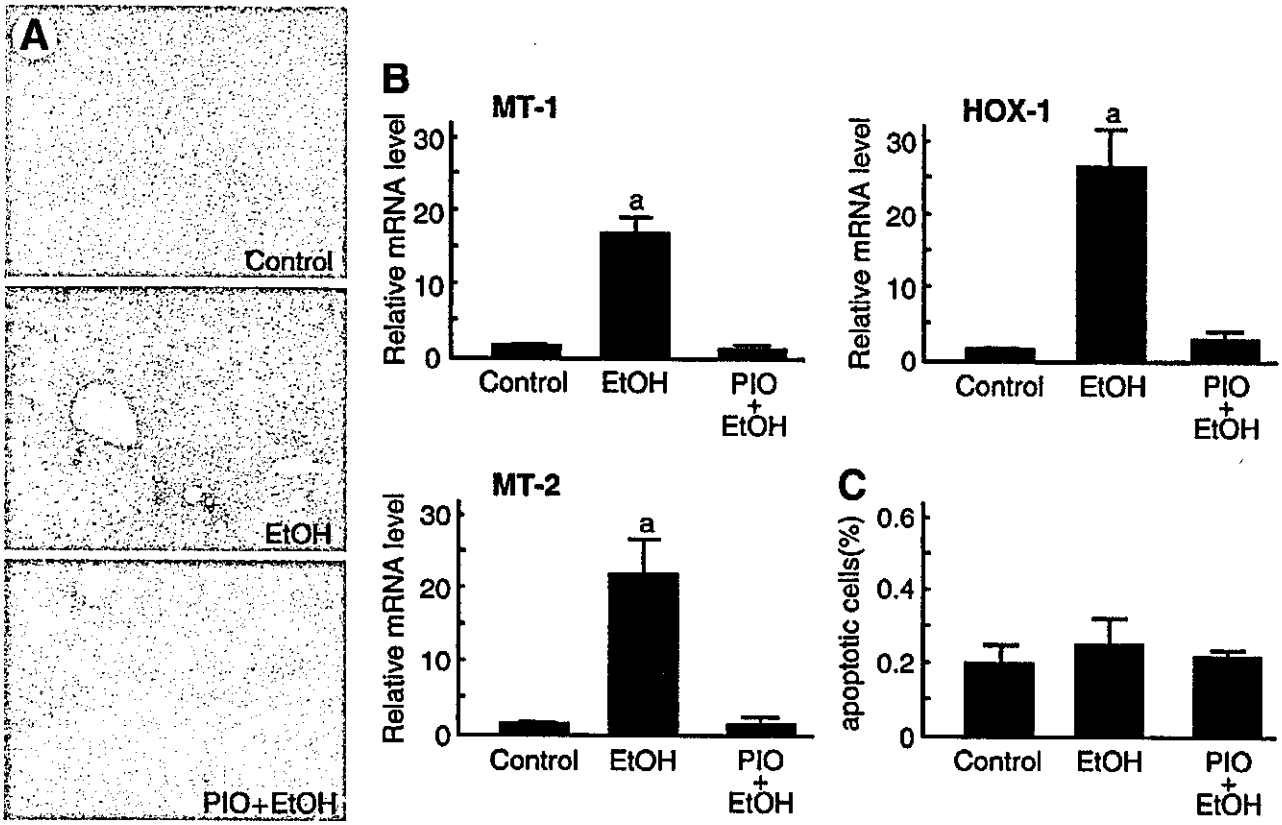

Figure 7. Effect of pioglitazone on hepatic lipid peroxidation, apoptosis, and expression of stress response proteins. (*A*) Immunohistochemistry for 4-HNE. Representative liver samples of control rat (Cont), ethanol-fed rats (EtOH), and ethanol-fed rats given pioglitazone (EtOH+Piog) (×100). (*B*) Real-time PCR analysis was used to assess stress response proteins such as MT-1, MT-2, and HOX-1 mRNA expression in liver homogenates among the groups. Results (and standard error of the mean) from 4 rats/group at the end of feeding period. All real-time quantitative PCR reactions were carried out in duplicate. $^{a}P < 0.05$ versus the other groups. (*C*) TUNEL results of liver apoptosis among the treated groups. The apoptotic cells and hepatocytes were counted from 5 lower microscopic fields for each animal.

substitute reagent that triggers lipid mobilization from the liver through stimulation of the c-Met pathway. As one might expect, the current results showed that pioglitazone mimics such effects of HGF to stimulate hepatic apoB synthesis and resultant VLDL secretion through HGF/c-Met intracellular signaling; this event could greatly contribute to mobilization of triglycerides from the liver undergoing chronic ethanol exposure.

Table 4. Blood Concentration of Ethanol and Acetaldehyde in Pioglitazone-Treated and Control Rats After Ethanol Administration (4 g/kg)

		Control	Pioglitazone Treated
Ethanol (mg/dL)	0 h	0 ± 0	0 ± 0
	2 h	184 ± 27	198 ± 26
	12 h	82 ± 22	84 ± 35
	24 h	3 ± 1	4 ± 2
Acetaldehyde (mg/L)	0 h	0 ± 0	0 ± 0
	2 h	1.9 ± 0.5	2.0 ± 0.4
	12 h	0.2 ± 0.1	0.2 ± 0.1
	24 h	0 ± 0	0 ± 0

Besides its action on lipid mobilization from the liver, pioglitazone obviously exerts its anti-steatotic actions through multiple mechanisms as judged by alterations in expression of genes responsible for triglyceride synthesis. SREBPs and stearoyl-CoA (SCD) are such genes responding to pioglitazone. Ntambi et al.[30] recently reported that a lipogenic diet fed to mice with a null mutation in the SCD1 gene (SCD1-/-) failed to induce the synthesis of triglycerides in liver, despite the induction of expression of SREBP-1 and its target genes. Cohen et al.[31] also reported that SCD-1 is required for the fully developed obese phenotype of leptin-deficient mice, including fatty liver. SCD-1 and SCD-2 catalyze the same reaction, and SCD-2 is reported to be expressed at higher levels in livers of mice overexpressing the truncated nuclear form of SREBP-1.[32] These observations suggest that induction of triglyceride synthesis is highly dependent on SCD

gene expression and that both SCD-1 and SCD-2 play a role in the mechanism of fatty liver. As shown in results from our and other laboratories, chronic ethanol feeding increased levels of SCD-2, and SREBP-1c expression. Consistent with our results, Crabb et al.[33] recently reported that chronic ethanol feeding activates hepatic SREBP-1. Such suppressive actions of pioglitazone on up-regulation of these genes could greatly improve ethanol-induced hepatic steatosis cooperatively with its aforementioned effects on the lipid mobilization via VLDL as a whole.

Recently, HGF was reported to prevent LPS-induced hepatic sinusoidal endothelial cell injury and intrasinusoidal fibrin deposition in rats.[34] It has also been reported that the mere presence of fat in the liver leads to hepatic lipid peroxidation and that chronic steatosis is associated with persistent lipid peroxidation.[35] Lipid peroxidation is proposed as a mechanism of alcohol-induced hepatotoxicity. It has been suggested that chronic lipid peroxidation could represent the missing link between chronic steatosis and steatohepatitis. In our study, pioglitazone improved ethanol-induced lipid peroxidation and resultant cellular damages by increasing the c-Met expression and by decreasing hepatic fat amounts, as indicated by results showing suppression of antioxidative genes such as MT-1, -2, and HOX-1.[36,37] Furthermore, so far as judged from the current TUNEL analyses, pioglitazone treatment did not induce any notable apoptosis in liver. Such a cytoprotective feature of pioglitazone on ethanol-induced hepatic steatosis is likely to be of great clinical advantage in that other thiazolidinedione derivatives such as troglitazone have been reported to induce apoptotic hepatocyte death, leading to a conflict for its clinical use.[38] Based on these findings, we propose an important new mechanism to explain the recovery from alcoholic fatty liver in response to pioglitazone (i.e., that pioglitazone enhances c-Met expression in hepatocytes, resulting in activation of HGF/c-Met signaling). The HGF/c-Met signaling activation induced by pioglitazone leads to increased apoB synthesis with subsequent lipid mobilization of VLDL from hepatocytes, and decreases hepatic SCD levels with decreased synthesis of triglycerides in liver. Such an effect of pioglitazone could also stimulate regeneration and attenuate lipid peroxidation.

The current study suggesting usefulness of pioglitazone to treat ethanol-induced hepatic steatosis led us to hypothesize that such an HGF-mimicking hepatoprotective PPARγ ligand could clinically be used to limit fatty infiltration of the liver caused by other disease conditions. For instance, posttransplant fatty infiltration in the donor liver accounts for a serious complication causing primary nonfunction.[39] Because use of steatotic livers are actually increasing for transplantation because of a shortage of the nonsteatotic donor grafts, we should find the method for amelioration of injury in donor fatty liver at liver transplantation. A possible use of the pioglitazone treatment deserves future studies if its use for posttransplanted recipients or for nonalcoholic steatohepatitis turned out to reduce the related liver injury. This may provide a means for designing future therapeutic strategies with pioglitazone. Pioglitazone may thus be useful as a therapeutic agent for alcoholic fatty liver and merits further evaluation.

References

1. Sorensen TI, Orholm M, Bentsen KD, Hoybye G, Eghoje K, Christoffersen P. Prospective evaluation of alcohol abuse and alcoholic liver injury in men as predictors of development of cirrhosis. Lancet 1984;2:241–4.
2. Teli MR, Day CP, Burt AD, Bennett MK, James OFW. Determinants of progression to cirrhosis or fibrosis in pure alcoholic fatty liver. Lancet 1995;346:987–990.
3. Lin HA, Yang SQ, Chuckaree C, Kuhajda F, Ronnet G, Diehl AM. Metformin reverses fatty liver disease in obese, leptin-deficient mice. Nat Med 2000;6:998–1003.
4. Zhou G, Myers R, Li Y, Chen Y, Shen X, Fenyk-Melody J, Wu M, Ventre J, Doebber T, Fujii N, Musi N, Hirshman MF, Goodyear LJ, Moller DE. Role of AMP-activated protein kinase in mechanism of metformin action. J Clin Invest 2001;108:1167–1174.
5. Shimabukuro M, Zhou YT, Lee Y, Unger RH. Troglitazone lowers islet fat and restores beta cell function of Zucker Diabetic Fatty rats. J Biol Chem 1998;273:3547–3550.
6. Higa M, Zhou YT, Ravazzola M, Baetens D, Orci L, Unger RH. Troglitazone prevents mitochondrial alterations, β cell destruction, and diabetes in obese prediabetic rats. Proc Natl Acad Sci U S A 1999;96:11513–11518.
7. Kakuma T, Lee Y, Higa M, Wang ZW, Pan W, Shimomura I, Unger RH. Leptin, troglitazone, and the expression of sterol regulatory element binding proteins in liver and pancreatic islets. Proc Natl Acad Sci U S A 2000;97:8536–8541.
8. Scheen AJ. Hepatotoxicity with thiazolidinediones: Is it a class effect? Drug Saf 2001;24:873–888.
9. Lieber CS, DeCarli LM, Sorrell MF. Experimental methods of ethanol administration. Hepatology 1989;10:501–510.
10. Maeshida Y, Kiyota Y, Yoshimura Y, Motohashi M, Tanayama S. Disposition of the new antidiabetic agent pioglitazone in rats, dogs, and monkeys. Arzneim.-Forsch/Drug Res 1997;47:29–35.
11. Hayakawa T, Shiraki T, Morimoto T, Shii K, Ikeda H. Pioglitazone improves insulin signaling defects in skeletal muscle from Wistar fatty (fa/fa) rats. Biochem Biophys Res Commun 1996;223:439–444.
12. Horikoshi H, Yoshioka T, Kawasaki T, Nakamura K, Matsunuma N, Yamaguchi K, Sasahara K. Troglitazone (CS-045), a new antidiabetic drug. Annu Rep Sankyo Res Lab 1994;46:1–57.
13. Tahara M, Matsumoto K, Nukiwa T, Nakamura T. Hepatocyte growth factor leads to recovery from alcohol-induced fatty liver in rats. J Clin Invest 1999;103:313–320.
14. Bachorik PS, Ross JW. National cholesterol education program recommendations for measurement of low-density lipoprotein cholesterol: executive summary. Clin Chem 1995;41:1414–1420.

15. Hatch FT, Lees RS. Practical methods for plasma lipoprotein analysis. Adv Lipid Res 1968;6:1–68.
16. Tomita K, Sato M, Kajiwara K, Tanaka M, Tamiya G, Makino S, Tomizawa M, Mizutani A, Kuwano Y, Shiina T, Ishii H, Kimura M. Gene structure and promoter for *Crad2* encoding mouse cis-retinol/3α-hydroxysterol short-chain dehydrogenase isozyme. Gene 2000;251:175–186.
17. Dunn JCY, Yarmush ML, Koebe HG, Tompkins RG. Hepatocyte function and extracellular matrix geometry: long-term culture in a sandwich configuration. FASEB J 1989;3:174–177.
18. Lawrence JM, Reckless JP. Actos (pioglitazone): a new treatment for type 2 diabetes. Hosp Med 2001;62:411–416.
19. Pelizzari CA, Khodarev NN, Gupta N, Calvin DP, Weichselbaum RR. Quantitative analysis of DNA array autoradiographs. Nucleic Acids Res 2000;28:4577–4581.
20. Tenenbaum SA, Carson CC, Lager PJ, Keene JD. Identifying mRNA subsets in messenger ribonucleoprotein complexes by using cDNA arrays. Proc Natl Acad Sci U S A 2000;97:14085–14090.
21. Okada T, Mizoi Y. Studies on the problem of blood acetaldehyde determination in man and level after alcohol intake. Jpn J Alcohol Drug Depend 1982;17:141–159.
22. Wright HM, Clish CB, Mikami T, Hauser S, Yanagi K, Hiramatsu R, Serhan CN, Spiegelman BM. A synthetic antagonist for the peroxisome proliferator-activated receptor gamma inhibits adipocyte differentiation. J Biol Chem 2000;275:1873–1877.
23. Levine JA, Harris MM, Morgan MY. Energy expenditure in chronic abuse. Eur J Clin Invest 2000;30:779–786.
24. Eaton S, Record CO, Bartlett K. Multiple biochemical effects in the pathogenesis of alcoholic fatty liver. Eur J Clin Invest 1997;27:719–722.
25. Michalopoulos GK, Defrances MC. Liver regeneration. Science 1997;276:60–66.
26. Stuart KA, Riordan SM, Lidder S, Crostella L, Williams R, Skouteris GG. Hepatocyte growth factor/scatter factor-induced intracellular signaling. Int J Exp Pathol 2000;81:17–30.
27. Takehara T, Nakamura T. Protective effect of hepatocyte growth factor on *in vitro* hepatitis in primary cultured hepatocytes. Biomed Res 1991;12:335–338.
28. Ishiki Y, Ohnishi H, Muto Y, Matsumoto K, Nakamura T. Direct evidence that hepatocyte growth factor is a hepatotropic factor for liver regeneration and has a potent antihepatitis effect in vivo. Hepatology 1992;16:1227–1235.
29. Kaibori M, Kwon AH, Oda M, Kamiyama Y, Kitamura N, Okumura T. Hepatocyte growth factor stimulates synthesis of lipids and secretion of lipoproteins in rat hepatocytes. Hepatology 1998;27:1354–1361.
30. Ntambi JM, Miyazaki M, Stoehr JP, Lan H, Kendziorski CM, Yandell BS, Song Y, Cohen P, Friedman JM, Attie AD. Loss of stearoyl-CoA desaturase-1 function protects mice against adiposity. Proc Natl Acad Sci U S A 2002;99:11482–11486.
31. Cohen P, Miyazaki M, Socci ND, Hagge-Greenberg A, Liedtke W, Soukas AA, Sharma R, Hudgins LC, Ntambi JM, Friedman JM. Role for stearoyl-CoA desaturase-1 in leptin-mediated weight loss. Science 2002;297:240–243.
32. Shimomura I, Shimano H, Korn BS, Bashmakov Y, Horton JD. Nuclear sterol regulatory element-binding proteins activate genes responsible for the entire program of unsaturated fatty acid biosynthesis in transgenic mouse liver. J Biol Chem 1998;273:35299–35306.
33. You M, Fischer M, Deeg MA, Crabb DW. Ethanol induces fatty acid synthesis pathways by activation of sterol regulatory element-binding protein (SREBP). J Biol Chem 2002;277:29342–29347.
34. Sato S, Kaido T, Yamaoka S, Yoshikawa A, Arii S, Nakamura T, Niwano M, Imamura M. Hepatocyte growth factor prevents lipopolysaccharide-induced hepatic sinusoidal endothelial cell injury and intrasinusoidal fibrin deposition in rats. J Surg Res 1998;80:194–199.
35. Letteron P, Fromenty B, Terris B, Degott C, Pessayre D. Acute and chronic hepatic steatosis lead to in vivo lipid peroxidation in mice. J Hepatol 1996;24:200–208.
36. Kyokane T, Norimizu S, Taniai H, Yamaguchi T, Takeoka S, Tsuchida E, Naito M, Nimura Y, Ishimura Y, Suematsu M. Carbon monoxide from heme catabolism protects against hepatobiliary dysfunction in endotoxin-treated rat liver. Gastroenterology 2001;120:1227–1240.
37. Hayashi S, Takamiya R, Yamaguchi T, Matsumoto K, Tojo SJ, Tamatani T, Kitajima M, Makino N, Ishimura Y, Suematsu M. Induction of heme oxygenase-1 suppresses venular leukocyte adhesion elicited by oxidative stress: role of bilirubin generated by the enzyme. Circ Res 1999;85:663–671.
38. Yamamoto Y, Nakajima M, Yamazaki H, Yokoi T. Cytotoxicity and apoptosis produced by troglitazone in human hepatoma cells. Life Sci 2001;70:471–482.
39. Imber CJ, Peter SDS, Handa A, Friend PJ. Hepatic steatosis and its relationship to transplantation. Liver Transpl 2002;8:415–423.

Received March 8, 2003. Accepted December 4, 2003.

Address reprint requests to: Hiromasa Ishii, M.D., Department of Internal Medicine, School of Medicine, Keio University, 35 Shinanomachi, Shinjuku-ku, Tokyo 160-8582, Japan. e-mail: hishii@sc.itc.keio.ac.jp; fax: (81) 3-3356-9654.

Supported by a grant from Keio University, School of Medicine, Nateglinide Memorial Toyoshima Research and Education Fund, and the 21st Century Center-Of-Excellence (COE) Program from Ministry of Education, Culture, Sports, Science, and Technology.

The authors thank T. Saito, H. Ochiai, M. Tomizawa, and E. Tokubo for technical assistance.

Kupffer Cells Alter Organic Anion Transport Through Multidrug Resistance Protein 2 in the Post–Cold Ischemic Rat Liver

Atsushi Kudo,[1,2] Satoshi Kashiwagi,[3] Mayumi Kajimura,[2] Yasunori Yoshimura,[3] Koji Uchida,[4] Shigeki Arii,[1] and Makoto Suematsu[2]

Although Kupffer cells (KCs) may play a crucial role in post–cold ischemic hepatocellular injury, their role in nonnecrotic graft dysfunction remains unknown. This study examined reveal the role of KC in post–cold ischemic liver grafts. Rat livers treated with or without liposome-encapsulated dichloromethylene diphosphonate, a KC-depleting reagent, were stored in University of Wisconsin (UW) solution at 4°C for 8 to 24 hours and reperfused while monitoring biliary output and constituents. The ability of hepatocytes to excrete bile was assessed through laser-confocal microfluorography *in situ*. Cold ischemia-reperfused grafts decreased their bile output significantly at 8 hours without any notable cell injury. This event coincided with impaired excretion of glutathione and bilirubin-IXα (BR-IXα), suggesting delayed transport of these organic anions. We examined whether intracellular relocalization of multidrug resistance protein-2 (Mrp2) occurred. Kinetic analyses for biliary excretion of carboxyfluorescein, a fluoroprobe excreted through this transporter, revealed significant delay of dye excretion from hepatocytes into bile canaliculi. The KC-depleting treatment significantly attenuated this decline in biliary anion transport mediated through Mrp2 in the 8-hour cold ischemic grafts via redistribution of Mrp2 from the cytoplasm to the canalicular membrane. Furthermore, thromboxane A_2 (TXA_2) synthase in KC appeared involved as blocking this enzyme improved 5-carboxyfluorescein excretion while cytoplasmic internalization of Mrp2 disappeared in the KC-depleting grafts. In conclusion, KC activation is an important determinant of nonnecrotic hepatocellular dysfunction, jeopardizing homeostasis of the detoxification capacity and organic anion metabolism of the post–cold ischemic grafts. (HEPATOLOGY 2004;39:1099–1109.)

Abbreviations: KC, Kupffer cell; UW solution, University of Wisconsin solution; BR-IXα, bilirubin-IXα; Mrp2, multidrug resistance protein 2; BC, bile canaliculi; TXA_2, thromboxane A_2; CF, carboxyfluorescein; ATP, adenosine triphosphate; TX, thromboxane; EHBRs, Eisai hyperbilirubinemia rats; LDD, liposome-encapsulated dichloromethylene diphosphonate; GSH, reduced glutathione; LDH, lactate dehydrogenase; cAMP, cyclic adenosine monophosphate; CFDA, carboxyfluorescein diacetate.

From the [1]Department of Hepatobiliary Pancreatic Surgery, School of Medicine, Tokyo Medical and Dental University, Bunkyo-ku, Tokyo, Japan; the Departments of [2]Biochemistry and Integrative Medical Biology and [3]Obstetrics and Gynecology, Keio University, School of Medicine, Tokyo, Japan; and the [4]Department of Food and Biodynamics, Graduate School of Bioagricultural Sciences, Nagoya University, Nagoya, Japan.

Received September 24, 2003; accepted December 23, 2003.

Supported, in part, by a grant from Keio University, School of Medicine, the 21st Century Center of Excellence Program, and the Leading Project for Biosimulation and Grant-in-Aid for Creative Science Research (13GS0015) from the Ministry of Education, Sciences, and Technology of Japan as well as by Advanced Medical Technology in Health Sciences Research Grants from Ministry of Health and Welfare in Japan.

Address reprint requests to: Makoto Suematsu, M.D., Ph.D., Professor and Chair, Department of Biochemistry and Integrative Medical Biology, Keio University, School of Medicine, 35 Shinanomachi, Shinjuku-ku, Tokyo 160-8582, Japan. E-mail: msuem@sc.itc.keio.ac.jp; fax: +81-3-3358-8138.

Published online in Wiley InterScience (www.interscience.wiley.com).

DOI 10.1002/hep.20104

Although use of University of Wisconsin (UW) solution has improved mean preservation time for liver transplantation, primary graft nonfunction and initial poor function still persist.[1–3] The clinical incidence of such dysfunction and the resultant lack of graft survival depend on storage time.[1–4] Reperfusion injury is the main cause of graft failure after prolonged cold ischemia.[5–9] During storage, hepatocytes swell and form blebs.[6–8] Upon reperfusion, however, these same changes in the parenchymal cells are restored without leading to irreversible injury.[6–8] On the other hand, sinusoidal endothelial cells lose their viability, and Kupffer cells (KCs) are activated.[6–10] According to previous studies using rat liver grafts stored in UW solution, the critical storage time at which changes in sinusoidal cells occur is longer than 16 hours.[6,7] In these grafts, cells were damaged to cause platelet trapping,[10] fibrin deposition,[11] and leukocyte margination.[12] In grafts stored for a shorter duration, hepatic adenosine triphosphate (ATP) content was reported to be well recovered after reperfusion, suggesting that parenchymal cells are viable.[13,14]

Otherwise, it has not been determined whether hepatocytes lose their functions without displaying irreversible injury and then interfere with the graft function as a whole. Although biliary output, clearance of taurocholate, and bromosulfophtalein have been measured in previous studies,[13–15] these studies failed to demonstrate such functional alterations in hepatocytes even when the storage time was extended to 18 hours.[13] Scant information is available regarding alterations in the ability of the post–cold ischemic grafts to excrete bile constituents. Such indices include the ability of hepatocytes to generate the osmotic driving force for bile formation and to excrete bile salts or organic anions; thus excretion of glutathione and bilirubin could serve as a marker for detecting early hepatocellular changes in the grafts. The ability to excrete organic anions could determine the efficiency of the graft to detoxify xenobiotics and the severity of post–cold ischemic hyperbilirubinemia, a risk factor for allograft dysfunction in clinical transplantation.[2,16]

We examined changes in constituents of bile samples as a function of storage time and revealed impaired excretion of glutathione and bilirubin as an early event on hepatocytes. This event turned out to be the result of cytoplasmic relocalization of multidrug resistance associated protein 2 (Mrp2), an ATP-dependent transporter for biliary excretion of the organic anions. Our results suggest that the function of this transporter is impaired, whereas the grafts apparently maintain their overall energy charges without showing any notable hepatocellular damage. Furthermore, mechanisms for such a change in hepatocytes appear to involve thromboxane (TX) synthesis in KCs from grafts exposed to a relatively short duration of cold ischemia (8 hours).

Materials and Methods

Animal Preparation. Experimental protocols were approved by the Animal Care Committee of Keio University School of Medicine in accordance with their institutional guidelines. Male Wistar rats (220–260 g, CLEA Japan, Tokyo) and Eisai hyperbilirubinemia rats (EHBRs) (220–260 g, Sankyo Inc., Tokyo) that had been allowed free access to laboratory chow and tap water were fasted 24 hours before experiments. Livers of these rats were perfused *ex vivo* with oxygenated Krebs-Henseleit buffer as the baseline perfusate[17,18] and stored in UW solution at 4°C for desired lengths of time.[14] When necessary, rats were pretreated with an intravenous injection of liposome-encapsulated dichloromethylene diphosphonate (LDD) 24 hours prior to preparation of the *ex vivo* liver perfusion for the cold storage according to our previous studies.[14,19] As described previously, this procedure eliminated KCs almost completely, as judged by immunohistochemistry.[20] After cold storage, the grafts were gently rinsed with a transportal injection of 40 mL of Krebs Ringer solution and perfused with the oxygenated buffer in the presence or absence of sodium taurocholate at 30 μmol/L at a constant flow (32 mL/min) in a single-pass mode.[14,21] For some experiments, either OKY-046, an inhibitor of thromboxane A_2 (TXA_2) synthase, or indomethacin, an inhibitor of cyclooxygenase, was added in UW solution as well as in the rinse solution at desired concentrations.[22]

Determination of Bile and Tissue Constituents. Bile samples were used to determine concentrations of total bile salts, phospholipids, reduced glutathione (GSH), and bilirubin-IXα (BR-IXα).[23,24] BR-IXα was determined by an enzyme-linked immunosorbent assay using 24G7.[24] This monoclonal antibody can recognize BR-IXα, the terminal heme-degrading product generated specifically through the HO reaction as described earlier.[24,25] Activities of lactate dehydrogenase (LDH) were measured as described earlier.[17] ATP in the liver grafts was determined by the luciferrin–luciferase method as described elsewhere.[14,21] Cyclic adenosine monophosphate (cAMP) in the grafts was determined by an enzyme-linked immunosorbent assay (Biotrak system, Amersham Biosciences, Buckinghamshire, United Kingdom).

Analyses of Biliary Excretion Rates of Carboxyfluorescein. Carboxyfluorescein (CF) is an organic anion *that* is excreted from various cells through Mrp2.[26,27] The ester precursor of this dye, CF diacetate (CFDA) was loaded transportally into the livers at 50 nmol/L for 10 minutes in the presence of 1.5 mmol/L probenecid, a potent inhibitor of Mrp2.[26,28] This reagent can enter hepatocytes and is hydrolyzed by esterase into CF to be excreted into bile.[14,17,29] After the 10-minute CFDA loading, the liver was perfused with the probenecid-free buffer to trigger the excretion of CF into bile. In the cold ischemic groups, the stored grafts were loaded with the CFDA containing buffer for 10 minutes in the presence of probenecid, followed by removal of probenecid and subsequent reperfusion for 50 minutes. Bile samples collected from these preparations were deep-frozen until the fluorescence measurements were made using a 96-well, multichannel fluorescence spectrophotometer. The measurements were performed under epi-illumination at 440 nm, the isosbestic wavelength of the dye, which yields fluorescence at 510 nm without interfering with the pH values of the samples.[26] The concentration of CF in samples was calibrated with known concentrations of CF dissolved in phosphate buffer saline. As seen later in the Results section, CF concentrations appeared to decline exponentially with time. With this assumption, biliary CF

lifetimes were determined as the $T_{1/2}$ of the exponential decay. Thus this method is insensitive to the initial amounts of CF loaded into the perfused liver.

In Situ *Visualization of Hepatocellular CF Exclusion.* Liver grafts loaded with CF using the aforementioned protocols were observed through intravital laser confocal microfluorography as described previously.[14,20,30] As shown later in the Results section, CF was notably loaded into hepatocytes in the presence of probenecid. Upon removal of the reagent, the dye was immediately excluded from hepatocytes, excreted into bile canaliculi (BC) to display honeycomb networks, and finally disappeared from the parenchyma. To examine if the dye exclusion depends on Mrp2 function, some grafts were reperfused with the buffer containing 1.5mmol/L probenecid. The laser confocal microfluorographs were captured by an inverted-type microscope (Diaphot 300, Nikon/Sankei, Tokyo, Japan) equipped with an intensified charged-coupled device (CCD) camera (C5810, Hamamatsu Photonics, Hamamatsu, Japan) and multi-pinhole laser confocal processor (CSU-10, Yokogawa Electric Co., Tokyo, Japan). All microfluorographs were digitally processed into 8-bit gray level images. To calibrate the fluorescence intensities, known concentrations of CF were prepared *in vitro* and the images were captured under the identical optical parameters of the camera. Gray levels in hepatocytes were measured by variable square window ($2 \times 2\ \mu m^2$) using a digital image processor.[18,31] At least 10 different hepatocytes in the microscopic fields of interest were analyzed in a single experiment. Assuming that fluorescence intensities measured at the liver surface is identical to those measured in the solution, gray levels were converted to apparent CF concentrations using the calibration line (designated as CFapp).

We also conducted morphometry to examine structural changes in BC networks as an index of hepatocellular damages. As shown later in the Results section, normally functioning hepatocytes were characterized by polygonal CF filling in surrounding BC, while those damaged were judged by partial disappearance of the surrounding BC network. The number of such intact hepatocytes surrounded by complete BC filling by CF was counted in the areas of interest. Approximately 0.05 mm^2 of the liver surface was analyzed in a single experiment for such evaluations.

Immunohistochemical Analyses of Subcellular Mrp2 Distribution. To evaluate Mrp2 in hepatocytes of the grafts, the liver samples were fixed, sliced, and stained with monoclonal antibody M_2III-6 according to a previous study.[32] The antigen on the sections was visualized using phycoerythrin-conjugated anti-mouse immunoglobulin G and was observed through laser confocal microfluorography at 488 nm as described elsewhere.[20,30] To examine BC localization and hepatocellular internalization of Mrp2, the sections were double-immunostained with a monoclonal antibody against ZO-1, another marker expressed in hepatocellular junction.[33] To determine changes in the protein distribution in a semiquantitative manner, single-stained microfluorographs of Mrp2 were converted as monochrome 8-bit images.[14] The gray levels (1–256) were measured at both cytoplasmic and canalicular domains in individual hepatocytes. At least five different sites for each domain were chosen in a single cell to calculate the relative values of cytoplasmic intensities versus the corresponding canalicular intensities. Such a measurement was made in 40 to 60 hepatocytes in four different grafts to construct histograms of the percentage of cytoplasmic intensities of Mrp2-associated immunoreactivities [defined as %I-Mrp2(cyt/bc)]. The elevation of this index represented an increase in Mrp2 internalization. The histograms were compared with the control grafts and those exposed to cold ischemia with and without the KC-depleting procedure in the presence or absence of the TXA_2 synthase inhibitor.

To examine differences in Mrp2 expression in the whole liver grafts among the groups, Western blot analyses were performed using the same monoclonal antibody. We also investigated alterations in oxidative modification of Mrp2 by immunoprecipitating the protein by the antibody M_2III-6 to follow Western analyses by an anti-acrolein monoclonal antibody (5F6).[34,35]

Statistical Analyses. The statistical significance of data among different experimental groups was determined by one-way ANOVA and Fischer's multiple comparison test. $P < .05$ was considered significant.

Results

Storage Time–Dependent Reduction of Bile Output in Liver Grafts. To test the viability of liver grafts, the release of LDH in the venous perfusate was measured as an index of cell lysis. As seen in Table 1, the grafts exposed to cold ischemia for less than 24 hours did not display any notable elevation of LDH. At 48 hours, the LDH release became evident at the beginning and end of the 60-minute reperfusion, showing that necrotic cell death was undetectable in cold ischemic grafts exposed less than 24 hours under the current experimental conditions. Figure 1 illustrates time courses of bile output as a function of reperfusion time in grafts undergoing varied lengths of cold ischemia. As seen in panel A, where sodium taurocholate was added, the grafts exposed to 8-hour ischemia increased their output to a level comparable to that in the controls at 30 minutes, but decreased it 50 to 60 minutes after the initial reperfusion. In the grafts exposed to pro-

Table 1. Effect of the Duration of Cold Preservation on the Release of LDH in the Venous Perfusate of the Grafts

Length of Cold Storage (Hrs)	5 Min-R	60 Min-R
Control	20 ± 6	35 ± 11
8	31 ± 7	25 ± 9
16	21 ± 8	34 ± 6
24	45 ± 8	43 ± 22
48	878 ± 377*	1206 ± 719*

Data represent means ± SE of measurements (mIU/min/g liver) from the grafts at the onset (0 min) and 60 min after the start of reperfusion (0-24 hrs; n = 5, 48 hrs; n = 3).

*$P < 0.05$ as compared with the value in other groups.

longed cold ischemia for 16 to 48 hours, such a reduction of output became further evident. Panel B shows the time course of bile recovery monitored in the absence of sodium taurocholate in the perfusate. The groups treated with cold ischemia for longer than 16 hours displayed significant decreases in output.

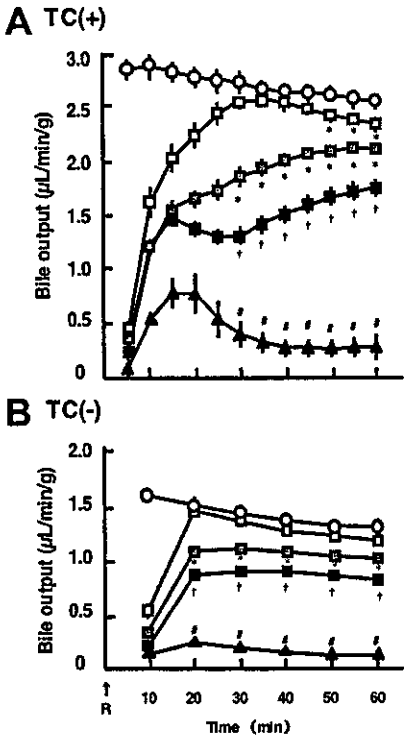

Fig. 1. Time courses of the bile output of liver grafts that have undergone cold preservation followed by reperfusion. Open circles denote the data from nonischemic control livers. Open, shaded, and closed squares indicate the data from grafts exposed to 8-, 16-, and 24-hour cold storage, respectively. Closed triangles indicate the data from 48-hour storage grafts. Values are mean ± SE of five separate experiments. TC (+) and TC (−): data collected in the presence and absence of sodium taurocholate at 30 μmol/L. R: the onset of reperfusion. Note that both bile salt-independent and -dependent outputs were decreased in the 16-hour preserved grafts. *$P < .05$ compared with the data from control. †$P < .05$ compared with the data from 16-hour grafts. #$P < .05$ compared with the data from 24-hour grafts.

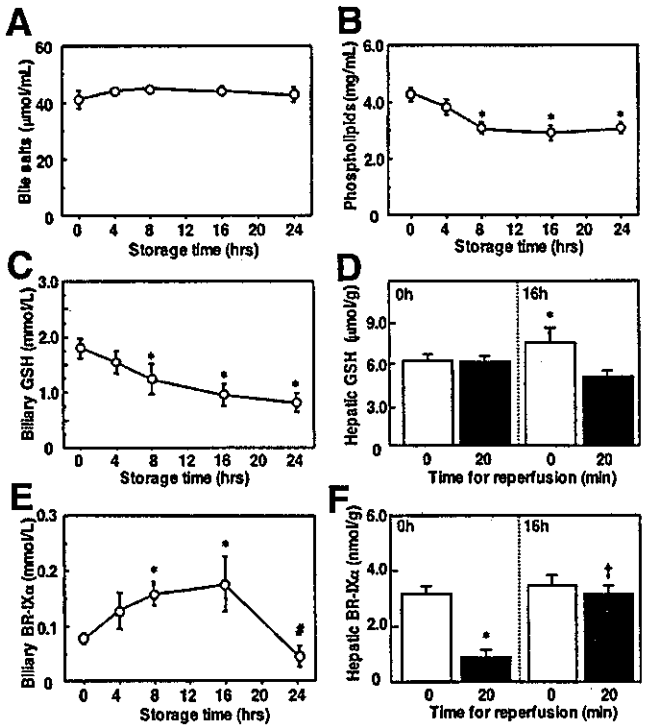

Fig. 2. Effects of duration of cold ischemia on biliary concentrations of bile constituents. Data of bile constituents were collected 20 minutes after the onset of reperfusion. (A) Bile salts. (B) Phospholipids. (C) Concentrations of reduced GSH in bile. (D) Hepatic content of GSH in the control and 16-hour stored grafts measured before and 20 minutes after reperfusion. (E) Concentrations of BR-IXα in bile. (F) Hepatic content of BR-IXα in the control and 16-hour stored grafts measured before and 20 minutes after reperfusion. Values are mean ± SE of five to seven separate experiments. *$P < .05$ compared with the data from control livers. #$P < .05$ compared with the data from the 16-hour group. †$P < .05$ compared with the data from the control grafts exposed to 20-minute reperfusion.

Alterations in Biliary Excretion of Glutathione and Bilirubin in Post-Cold Ischemic Livers. Observation of a significant decrease in bile flow in the grafts undergoing 16- and 24-hour cold ischemia led us to determine which bile constituents were responsible for cholestatic changes. Figure 2 presents data of bile constituents measured 20 minutes after the onset of reperfusion that were plotted as a function of storage time for cold ischemia. Concentrations of bile salts did not exhibit any significant reduction in any length of storage time, while those of phospholipids displayed notable reduction in both concentrations and fluxes in the group exposed to 8- to 24-hour cold ischemia (Fig. 2A, B). Considering that phospholipids are primarily excreted from hepatocytes into biliary compartments, these data suggest the presence of hepatocellular dysfunction in the grafts stored for more than 8 hours.

We next examined biliary excretion of GSH (Fig. 2C). Biliary concentrations in GSH were significantly reduced at 8 hours and declined as a result of the cold storage time.

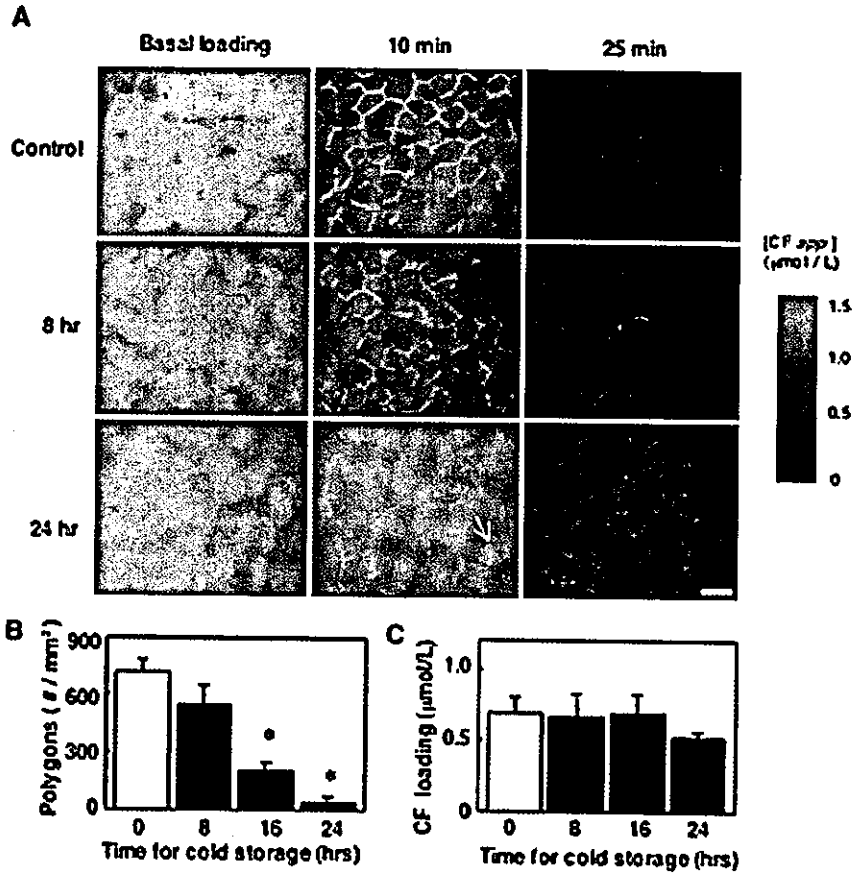

Fig. 3. Alterations in dynamics of hepatocellular CF excretion into BC in cold ischemia-reperfused grafts. (A) Representative pictures of the canalicular CF excretion captured before (Basal loading), and 10 minutes and 25 minutes after removal of probenecid. Note disruption of honeycomb patterns of BC networks in the 24-hour cold ischemic-reperfused graft (**arrow**). Color bar indicates the fluorescence intensities calibrated with known concentrations of CF (bar = 30 μm). (B) Differences in reperfusion-induced disruption of BC networks as judged by the density of CF-filled polygons in the grafts stored for varied duration of cold ischemia. $^*P < .05$ compared with the data from control livers. (C) Initial hepatocellular CF concentrations showing comparable CF loading among groups. Values are mean ± SE of five separate experiments.

We then examined the hepatic content of GSH; as seen in Fig. 2D, hepatic GSH content did not change before or after 20-minute reperfusion. In the grafts stored for 16 hours, the content apparently increased as a result of the use of UW solution containing GSH; upon 20-minute reperfusion, however, the content was rapidly repressed to the control level as GSH was removed from circulation, showing that the 20-minute reperfusion following 16-hour cold ischemia does not change the basal GSH content in the grafts. These results suggest that the decrease in biliary GSH excretion in the post–cold ischemic livers results from impairment of its transport to bile rather than from its reduction in the grafts, as long as the storage time was less than 16 hours. Because GSH is excreted through Mrp2, we next examined alterations in biliary concentrations of BR-IXα, a bile pigment excreted through the same transporter. As seen in Fig. 2E, the biliary concentration of BR-IXα in the initial 20-minute reperfusion was significantly elevated in the 8-hour ischemic group and reached its maximum in the 16-hour storage group. Finally, in the grafts undergoing 24-hour cold ischemia, initial concentrations of BR-IXα were abruptly decreased. Figure 2F illustrates the ability of the grafts to eliminate endogenous BR-IXα into bile. As seen in the control grafts, hepatic content of this bile pigment significantly decreased within the initial 20-minute perfusion. On the other hand, the same duration of reperfusion did not cause such a decrease in the 16-hour treated grafts. These results suggest that the ability of the 16-hour grafts to generate BR-IXα *de novo* surpasses their capacity to excrete the pigment into bile.

Global and Local Assessment of Mrp2 Function by CF Exclusion. Alteration in biliary excretion of GSH and BR-IXα raised the possibility that the ability of Mrp2 to eliminate these organic anions from hepatocytes could be impaired in grafts exposed to prolonged cold ischemia. However, because initial amounts of glutathione and BR-IXα were different among groups, measuring biliary excretion of these endogenous anions did not allow us to make a fair comparison of the organic anion-excreting ability of the grafts. To overcome this difficulty, the grafts were loaded with CF, an exogenous organic anion, and its elimination from hepatocytes into bile was examined. As seen in the left panels of Fig. 3A, hepatocellular CF loading appeared comparable among the grafts exposed to different lengths (0–24 hours) of cold ischemia. This was confirmed by the fluorescence intensitometry in Fig. 3C, indicating that the hepatocytes were viable. This was also consistent with results showing no notable release of LDH (Table 1). Immediately after the removal of probe-

necid, an inhibitor of Mrp2, CF loaded in hepatocytes was rapidly excreted into BC, forming honeycomb networks over the lobule within 10 minutes (Fig. 3A, middle column). At 25 minutes (Fig. 3A, right column), little fluorescence inside the cytoplasm became detectable, if any. In grafts that underwent cold ischemia reperfusion, two major changes in biliary CF excretion occurred: retardation of hepatocellular dye exclusion as judged by an elevation of the basal fluorescence at 25 minutes, and disappearance and deformation of bile canalicular networks as indicated in micrographs collected at 10 minutes. These changes became evident in grafts exposed to extended cold ischemia for 24 hrs (the bottom row in Fig. 3A).

Careful scanning at the site of BC in these microfluorographs captured at 10 minutes showed minimal but notable changes in the structure of the canalicular networks. As seen in Fig. 3B, the number of hepatocytes that were completely surrounded by CF-filled BC decreased as the duration of cold ischemia increased. Such a reduction of polygons became readily apparent in the grafts stored for 16 hours. Because the initial CF loading in hepatocytes was comparable in a range between 0 and 24 hours of ischemic duration, morphologic changes in BC appeared to occur initially at 16-hour cold ischemia. In other words, grafts exposed to 8-hour cold ischemia did not exhibit any significant changes in the morphology of BC networks.

The delay of CF exclusion was further examined in a quantitative manner by monitoring temporal alterations in the fluorescence of the graft hepatocytes (Fig. 4A). When probenecid was perfused continuously, the dye stayed in the cells, exhibiting a slight decline without showing canalicular excretion. As plotted in Fig. 4B, gray levels measured in hepatocytes allowed us to determine the $T_{1/2}$ of the CF exclusion from hepatocytes. Figure 4C illustrates $T_{1/2}$ values among the groups. In the absence of probenecid, $T_{1/2}$ was approximately 6 minutes, while in the presence of probenecid the decay was substantially slowed, suggesting near complete inhibition of Mrp2 transport. $T_{1/2}$ of the 8-hour cold ischemic graft to excrete CF was significantly greater, ranging midway between the control value and that measured in livers of EHBRs. It could be speculated that the smaller $T_{1/2}$ values in this mutant species compared with the probenecid-treated group is due to compensatory excretion of the dye through Mrp3 into the sinusoidal space.[36]

Effects of KC Depletion on Biliary CF Excretion in 8-hour Cold Ischemic Grafts. We attempted to evaluate the ability of the 8-hour cold ischemic grafts as a whole to excrete CF. To this end, the $T_{1/2}$ values for the dye exclusion were determined (Fig. 5). After removal of probenecid (T_0 in

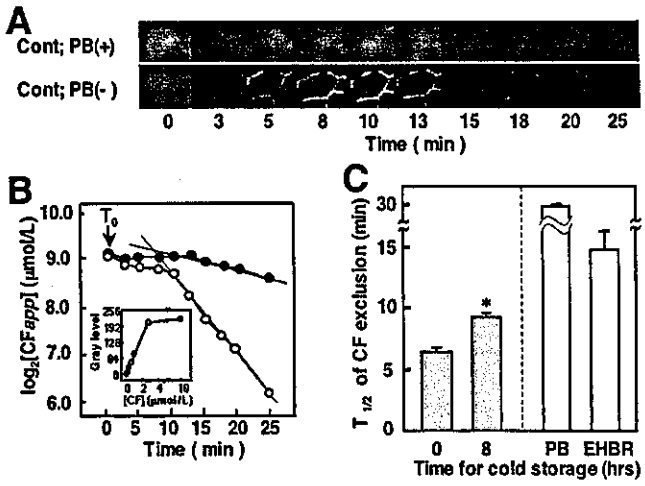

Fig. 4. *In vivo* quantitative analyses of Mrp2 function by visualizing BC excretion of CF. (A) Representative series of pictures showing the dye excretion from individual hepatocytes. Upper section: images from a graft perfused in the presence of 1.5 mM probenecid [PB(+)]. Lower section: images captured after the removal of probenecid [PB(−)]. Note the time-dependent reduction of fluorescence in the cells followed by condensation and disappearance of the dye in surrounding BC. The dye retention in the cells should also be noted. (B) The decay of hepatocellular CF fluorescence. Hepatocellular CF concentrations in the grafts treated with (**closed circles**) or without (**open circles**) probenecid were plotted semilogarithmically against the time so that a straight line represents an exponential curve. Inset: the calibration curve indicating the relationship between concentrations of CF and 8-bit gray levels. [CFapp]: apparent concentrations of CF. CF concentrations were linearly related to gray levels at concentrations less than 3 μmol/L ($r^2 = 0.996$, $P < .05$). (C) Differences in half-life time ($T_{1/2}$) of CF exclusion from hepatocytes. Values are mean ± SE of five separate experiments in each group. *$P < .05$ compared with the data from control livers. EHBR: grafts isolated from Eisai hyperbilirubinemia rats. PB: grafts perfused with 1.5 mM probenecid.

Fig. 5A), the CF concentrations in bile transiently increased and gradually returned to the basal level. Such a transient increase was not observed either in the presence of probenecid (shaded circles), or in the grafts isolated from EHBRs (closed circles), suggesting that Mrp2 is responsible for biliary CF excretion. When the CF exclusion was analyzed in the whole liver grafts stored for 8 and 16 hours, the decay appeared to be slower than that of the controls. Using the data collected from the 8-hour ischemic grafts, logarythmic values of the CF concentrations versus those at the peak (10 minutes) in bile samples were replotted as a function of reperfusion time (Fig. 5B). The $T_{1/2}$ values of the dye exclusion were then compared between the grafts treated with and without the KC depletion. In the livers untreated with LDD [KC(+)], the 8-hour cold ischemia exhibited prolonged $T_{1/2}$ values compared with the controls. Such a difference in $T_{1/2}$ between the two groups completely disappeared in the KC-depleting grafts. It is noteworthy that in the non–cold ischemic control livers, the KC-depleting procedure by itself did not alter the $T_{1/2}$ values; this indicates that the ameliorating

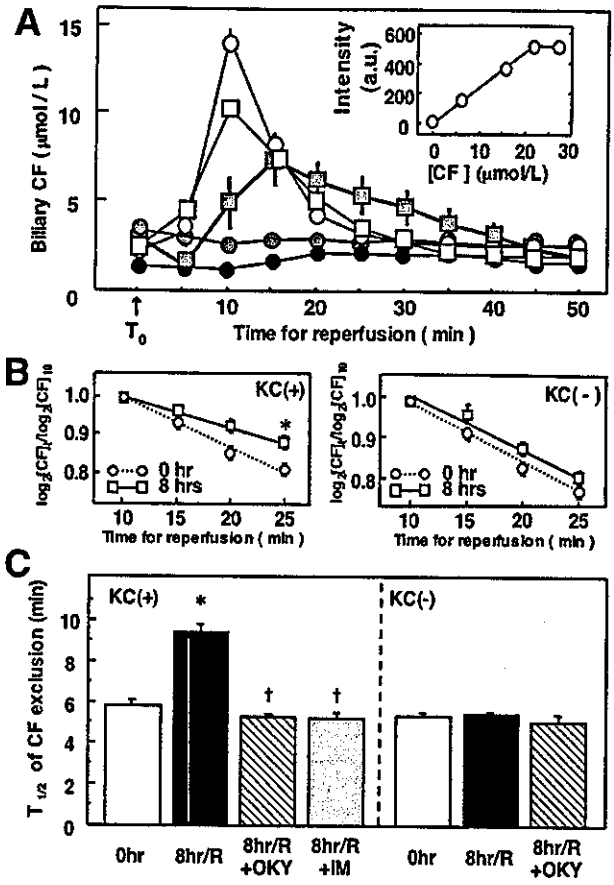

Fig. 5. Alterations in the ability of liver grafts to excrete CF into bile upon cold ischemia reperfusion. (A) Differences in time course of the biliary CF excretion in grafts exposed to varied lengths of cold ischemia. Open circles: control grafts perfused right after removing 1.5 mM probenecid, an Mrp2 inhibitor. Open and shaded squares: grafts undergoing 8- and 24-hour cold storage followed by reperfusion in the absence of probenecid, respectively. Shaded circles: grafts normoperfused in the presence of probenecid. Closed circles: normoperfused grafts isolated from EHBRs. Values are mean ± SE of five separate experiments. T_0: time when probenecid was removed from the perfusate. Inset: a linear relationship between the CF concentration and fluorescence intensities. (B) Alterations in relative CF concentrations in bile collected at varied duration of reperfusion and effects of the depletion of KCs. Left: differences in the decay of biliary CF excretion between control (**broken lines**) and 8-hour stored liver grafts (**solid lines**). Right: effects of KC depletion by intravenous LDD. Open circles: control (**broken lines**). Open squares: 8-hour stored grafts (**solid lines**). Data represent mean ± SE of measurement from four separate experiments. $^*P < .05$ compared with the decays of CF exclusion in control livers. (C) Effects of KC depletion [KC(−)] by LDD and/or treatment with OKY-046 (OKY), an inhibitor of TXA_2 synthase, on lengthening $T_{1/2}$ values in the 8-hour cold storage livers. IM: indomethacin. Concentrations of OKY-046 and indomethacin in the storage and rinse solutions were 240 and 28 μmol/L, respectively. Note that an inhibitory action of OKY-046 disappears in the KC-depleting grafts. Values are mean ± SE of five to six separate experiments. $^*P < .05$ compared with the data from control livers. $^\dagger P < .05$ compared with the data in the 8-hour stored grafts.

effect of the KC depletion became evident only when the grafts experienced cold ischemia reperfusion.

To reveal mechanisms through which KCs in the 8-hour cold ischemic grafts caused prolonged CF excretion through Mrp2, we examined the involvement of TX, a major prostanoid released from activated KCs under post–cold ischemic conditions.[37,38] To this end, the effects of OKY-046, an inhibitor of TXA_2 synthase, were examined. As seen in Fig. 5C, application of this reagent at 240 μmol/L to the storage and rinse solutions abolished an increase in $T_{1/2}$ values of the CF exclusion almost completely. Because the TXA_2 synthase inhibitor might increase availability of arachidonic acid to synthesize other prostanoids (*e.g.*, PGE_2 and $PGF_{2\alpha}$), we examined if indomethacin, an inhibitor that suppresses all the prostanoids produced via the cyclooxygenase pathway (including TX) could attenuate or aggravate the $T_{1/2}$ values. As shown, this inhibitor also attenuated the prolonged $T_{1/2}$ values almost completely. Furthermore, effects of OKY-046 on the 8-hour cold ischemic grafts disappeared when KC was depleted, suggesting that the involvement of TX is KC-dependent.

Intracellular Relocalization of Mrp2 by 8-hour Cold Ischemia and Its Attenuation by KC Depletion. Because KCs are known to down-regulate Mrp2 in endotoxin-treated livers,[39] we examined if such a change could be involved in the mechanisms for the dysfunction of the transporter. As shown by Western blot analysis, amounts of Mrp2 protein were unchanged in the 8-hour cold ischemic grafts (Fig. 6A) as well as in the 24-hour ischemic grafts (data not shown). We also examined if the protein by itself was oxidatively modified as a consequence of postischemic oxidative insults. However, no apparent changes were found as judged by immunoprecipitation using the anti-acrolein antibody. An examination was then performed to determine whether or not hepatocellular localization of the protein is modified in the 8-hour cold ischemic grafts. As seen in Fig. 6B, its localization in BC was markedly reduced, while the background fluorescence in cytoplasm of hepatocytes was elevated in the 8-hour ischemia-reperfused grafts. As seen in the lower panels of Fig. 6, double-immunostaining with ZO-1 (green) revealed that colocalization of Mrp2 (red) in BC was markedly disrupted, while its intensities in the cytoplasm were elevated, suggesting the internalization of the protein. Such changes were attenuated in the grafts treated with KC depletion or OXY-046. The %I-Mrp2(cyt/bc) values—an index for internalization—indicated that the 8-hour cold ischemia-reperfusion significantly enhanced the Mrp2 internalization and that treatment with KC depletion or with blockade of TXA_2 synthase improved BC relocalization of the transporter.

We identified differences in the hepatic contents of ATP and cAMP in the KC(+) and KC(−) grafts after the 8-hour cold ischemia-reperfusion, but there was no notable significance between the two groups (3.4 ± 0.9 vs. 2.9 ± 1.1 μmol/g liver in ATP content and 8.9 ± 1.0 vs. 9.2 ± 0.5 pmol/g liver in cAMP content). These results

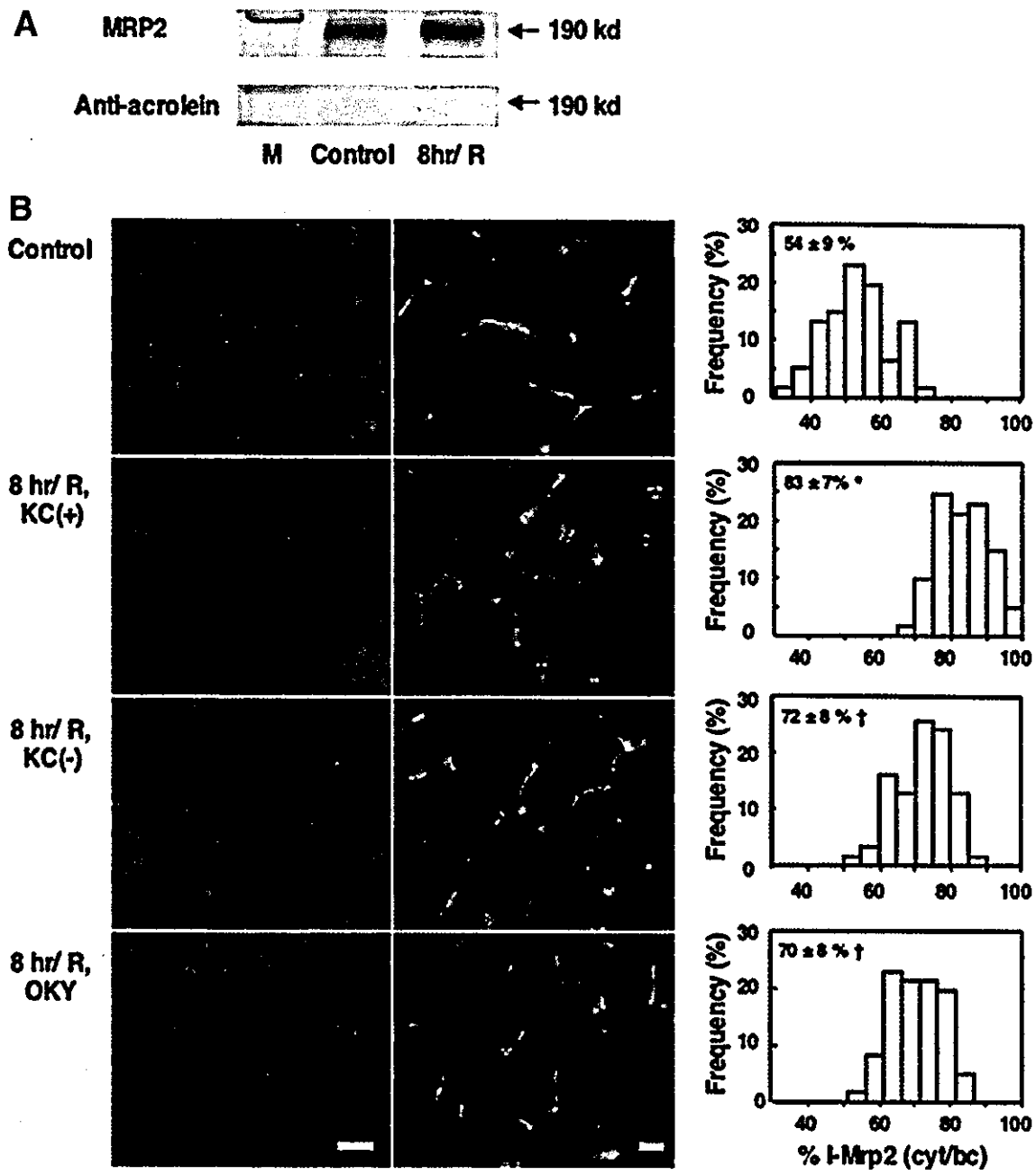

Fig. 6. Disruption of intracellular distribution of Mrp2 in liver grafts exposed to 8-hour cold ischemia and 60-minute reperfusion (8-hour/R), and effects of KC-depleting procedure [KC(−)] or treatment with OKY-046 (OKY). (A) Western blot analysis and immunoprecipitation of Mrp2 by the anti-acrolein monoclonal antibody (5F6). M: molecular marker. (B) Immunofluorescence analysis of Mrp2 distribution. Left: single staining with the anti-Mrp2 monoclonal antibody (M_2III-6) labeled with phycoerythrin (bar = 30 μm). Right: double immunostaining with the FITC-labeled ZO-1 antibody and the phycoerythrin-labeled M_2III-6 antibody (bar = 10 μm). (C) Semiquantitative analyses of hepatocellular Mrp2 localization. %I-Mrp2(cyt/bc); cytoplasmic intensities of Mrp2-associated immunoreactivities versus those measured at BC. Values are mean ± SE of measurements in 40 to 60 hepatocytes/graft from four separate livers. *$P < .05$ compared with the data from control livers. †$P < .05$ compared with the data collected from the 8-hour/R-KC(+) group.

suggest that amelioration of intracellular retrieval of this ATP-binding protein by the KC depletion did not result from alterations in tissue contents of ATP and cAMP.

Discussion

This study provided evidence that the impaired ability of hepatocytes to carry out the Mrp2-dependent excretion of organic anions is an early event during graft dysfunction caused by cold ischemia, followed by a short duration of reperfusion. This change in hepatocytes was subtle and not associated with necrosis; nevertheless, it was critical enough to cause an imbalance between the cellular generation and excretion of glutathione and bilirubin at the level of the whole graft. Extending the duration of cold